Steel and Composite Structures, *Vol. 33, No. 1 (2019) 93-109*
DOI: https://doi.org/10.12989/scs.2019.33.1.093

Vibration analysis of double-bonded micro sandwich cylindrical shells under multi-physical loadings

Raziye Yazdani [1], Mehdi Mohammadimehr*[1] and Ashraf M. Zenkour [2,3]

[1] *Department of Solid Mechanics, Faculty of Mechanical Engineering, University of Kashan, P.O. Box: 87317-53153, Kashan, Iran*
[2] *Department of Mathematics, Faculty of Science, King Abdulaziz University, P.O. Box 80203, Jeddah 21589, Saudi Arabia*
[3] *Department of Mathematics, Faculty of Science, Kafrelsheikh University, Kafrelsheikh 33516, Egypt*

(*Received February 7, 2019, Revised September 17, 2019, Accepted September 29, 2019*)

Abstract. In the present study, vibration analysis of double bonded micro sandwich cylindrical shells with saturated porous core and carbon/boron nitride nanotubes (CNT/BNNT) reinforced composite face sheets under multi-physical loadings based on Cooper-Naghdi theory is investigated. The material properties of the micro structure are assumed to be temperature dependent, and each of the micro-tubes is placed on the Pasternak elastic foundations, and mechanical, moisture, thermal, electrical, and magnetic forces are effective on the structural behavior. The distributions of porous materials in three distributions such as non-linear non-symmetric, nonlinear-symmetric, and uniform are considered. The relationship including electro-magneto-hydro-thermo-mechanical loadings based on modified couple stress theory is obtained and moreover the governing equations of motion using the energy method and the Hamilton's principle are derived. Also, Navier's type solution is also used to solve the governing equations of motion. The effects of various parameters such as material length scale parameter, temperature change, various distributions of nanotube, volume fraction of nanotubes, porosity and Skempton coefficients, and geometric parameters on the natural frequency of double bonded micro sandwich cylindrical shells are investigated. Increasing the porosity and the Skempton coefficients of the core in micro sandwich cylindrical shell lead to increase the natural frequency of the structure. Cylindrical shells and porous materials in the industry of filters and separators, heat exchangers and coolers are widely used and are generally accepted today.

Keywords: free vibration analysis; double-bonded micro sandwich shell; porous media; composite; CNT/BNNT; various physical parameters

1. Introduction

Sandwich cylindrical shell structure has been used widely in various micro-thermo-mechanical systems due to their unique features including couple thermal and mechanical properties and to optimum conditions for dynamic behavior, strength and stability. Many studies have been performed to deduce the vibration of such three-layer cylindrical shells with soft cores. Loy *et al*. (1997) studied the analysis of cylindrical shells using an improved version of the generalized differential quadrature (GDQ) method. Akbari Alashti and Khorsand (2012) presented 3D elastic analysis for functionally graded (FG) cylindrical shells bonded with piezoelectric layers subjected to dynamic and thermal loadings. Yang *et al*. (2014) investigated the vibration and damping characteristics of free–free composite sandwich cylindrical shell with pyramidal truss-like cores using the Rayleigh–Ritz model and finite element method. Zeighampour and Beni (2014) discussed the cylindrical thin-shell model based on modified strain gradient theory. They used the thin shell theory based on modified strain gradient theory.

*Corresponding author, Ph.D., Associate Professor,
E-mail: mmohammadimehr@kashanu.ac.ir

In the present decades, thermo-mechanical stress analysis for thick-walled cylinder has been investigated. Beni *et al*. (2015) presented the size-dependent equations of motion for FG cylindrical shell using shear deformation model and rotation inertia. Bahadori and Najafizadeh (2015) discussed the dynamic behavior of FG cylindrical shell surrounded by two-parameter elastic foundation based on the first-order shear deformation shell theory (FSDT) by using the general differential quadrature (GDQ) method. They concluded that their analysis may be extended to study the influence of boundary conditions on shell vibrations by the higher-order shear deformation shell theory (HSDT). Dey and Ramachandra (2016) presented the non-linear dynamic response of laminated composite circular cylindrical shell under periodic radial point loading and static axial partial loading. They considered the von Kármán type of non-linearity and used Donnell's shell theory based on FSDT. Razavi *et al*. (2016) presented the electromechanical vibration of cylindrical nanoshell made of FG piezoelectric material (FGPM) using the consistent couple stress theory and the cylindrical shell model. Shen *et al*. (2018) studied the small and large amplitude vibration behaviors of graphene-reinforced composite (GRC) laminated cylindrical panels supported by an elastic foundation under thermal environmental conditions.

Due to excellent mechanical, electrical and thermal

Copyright © 2019Techno-Press, Ltd.
http://www.techno-press.org/?journal=scs&subpage=6
ISSN: 1229-9367 (Print), 1598-6233 (Online)

properties of carbon nanotubes (CNTs), such as high strength, high stiffness and high aspect ratio with low density, carbon nanotube-reinforced FG composites composed of these advanced materials have found wide applications as structural members in modern industries such as mechanical and aerospace engineering. Mohammadimehr *et al*. (2011) used the nonlocal elasticity theory to develop the elastic buckling of double-walled carbon nanotubes (DWCNTs) embedded in an elastic medium under axial compression. Arani *et al*. (2011) presented the stress analysis of a long piezoelectric polymeric hollow cylinder reinforced with CNT under combined magneto-thermo-electro-mechanical loading is investigated. Murmu *et al*. (2012) studied the effect of a longitudinal magnetic field on the transverse vibration of a magnetically sensitive DWCNT. Ghorbanpour Arani *et al*. (2012a) discussed the electro-thermal transverse vibration behavior of DWCNTs embedded in a surrounded elastic medium using nonlocal piezo-elasticity cylindrical shell theory. Arani *et al*. (2012b) presented the nonlinear vibrations analysis for multi-walled carbon nanotubes embedded in an elastic medium. Arani *et al*. (2015) discussed the static stresses analysis of CNT reinforced composite cylinder. Non-axisymmetric thermo-mechanical loadings are applied in presence of uniform longitudinal magnetic field and radial electric field.

Lei *et al*. (2015) investigated the free vibration of CNT reinforced FG rotating cylindrical panels. They used the element-free kernel particle (kp)-Ritz method to perform this analysis. Duc *et al*. (2015a) investigated mechanical and thermal stability of eccentrically stiffened functionally graded conical shell panels resting on elastic foundations and in thermal environment. Kheibari and Beni (2016) presented the free vibration of piezoelectric nanotubes based on Love's cylindrical thin-shell model by using couple stress theory. Pourasghar and Chen (2016) used the 3D elasticity theory to investigate the free vibration response of a CNT reinforced cylindrical panel resting in two-parameter elastic foundation in thermal environments. Song *et al*. (2016) presented the vibration characteristics of CNT reinforced FG composite closed cylindrical shells. They considered the thermal effect and used Reddy's high-order shear deformation theory. Mohammadimehr and Mehrabi (2017) presented the free vibration and stability analyses of double-bonded micro composite sandwich cylindrical shells reinforced by CNTs conveying fluid flow under magneto-thermo-mechanical loadings using modified couple stress theory based on Reddy's cylindrical double-shell theory. Duc *et al*. (2017) presented static response and free vibration of functionally graded carbon nanotube-reinforced composite rectangular plates resting on Winkler-Pasternak elastic foundations. Van Do *et al*. (2017) considered analysis of bi-directional functionally graded plates by FEM and a new third-order shear deformation plate theory. Sobhy and Zenkour (2018) investigated the effect of the magnetic field on the thermomechanical buckling and vibration of viscoelastic sandwich nanobeam of a homogeneous core integrated with two FG CNT reinforced face sheets and imposed in a humid environment. Mehar *et al*. (2017) investigated nonlinear thermoelastic frequency analysis of functionally graded carbon nanotubes-reinforced single/doubly curved shallow shell panels by finite element method. Some studies are illustrated about nonlinear static, buckling, vibration and dynamic responses on micro/nano structures (Duc 2014, Duc *et al*. 2016, Vuong and Duc 2018, Duc *et al*. 2015b, 2016, Minh and Duc 2019, Khoa *et al*. 2019, Nguyen *et al*. 2019).

Recently, many efforts have been made to develop various classes of porous structures. Poro material structures, such as beams, plates, and shells are widely used in structural design problems. In most problems of porous structures, the material properties vary through the thickness with a specific function (Barati *et al*. 2016, 2017, Barati and Zenkour 2018, Zenkour 2015, 2018, Yuan and Kardomateas 2018, Frostig *et al*. 2018). Jabbari *et al*. (2013) presented the buckling analysis of radially solid circular plate made of porous material bounded with the layers of piezoelectric actuators. Wang and Wu (2017) presented the free vibration analysis of a FG porous cylindrical shell subject to different sets of immovable boundary conditions. Also, some researchers worked about size dependent and surface effects on micro/nano structures (Liu *et al*. 2017a, b, 2019, Yu *et al*. 2019a, b).

Piezomagnetic and piezoelectric materials, nanotechnology and micro scale analysis for smart structures were investigated in the introduction. According to reviewed literature, a combination of these topics for smart double bonded sandwich cylindrical shell under multi-physical fields including mechanical, moisture, thermal, electrical, and magnetic loadings as well as three distributions of porous materials such as non-linear non-symmetric, nonlinear-symmetric, and uniform based on Cooper-Naghdi theory is a lack of study. Therefore, the novelty of this research is the free vibration analysis of double bonded micro sandwich cylindrical shells with saturated porous core and CNT/BNNT reinforced composite face sheets under various physical parameters including hydro-thermo-mechanical loadings based on Cooper-Naghdi theory. The distribution of porous materials in three distributions such as non-linear-non-symmetric porosity, nonlinear-symmetric of porosity, and uniform are taken into account. The relationships including electro-magneto-hydro-thermo-mechanical loadings together modified couple stress theory are obtained. Moreover, by the energy method and the Hamilton's principle, the governing equations of motion are derived. And then the Navier's analytical solution method is used to solve these equations. The results of the present research can be used for micro sandwich cylindrical shell with porous core in filtering liquids. Moreover, the porous materials as advanced engineering materials in aerospace, civil constructions and automotive industry especially as a core of sandwich structures due to their excellent multi functionality offered by low specific weight, efficient capacity of energy dissipation, reduced thermal and electrical conductivity, and enhanced recyclability. Design more smart structures under multi-physical fields includinghydro-thermo-mechanical loadings is one of the other applications of this study results.

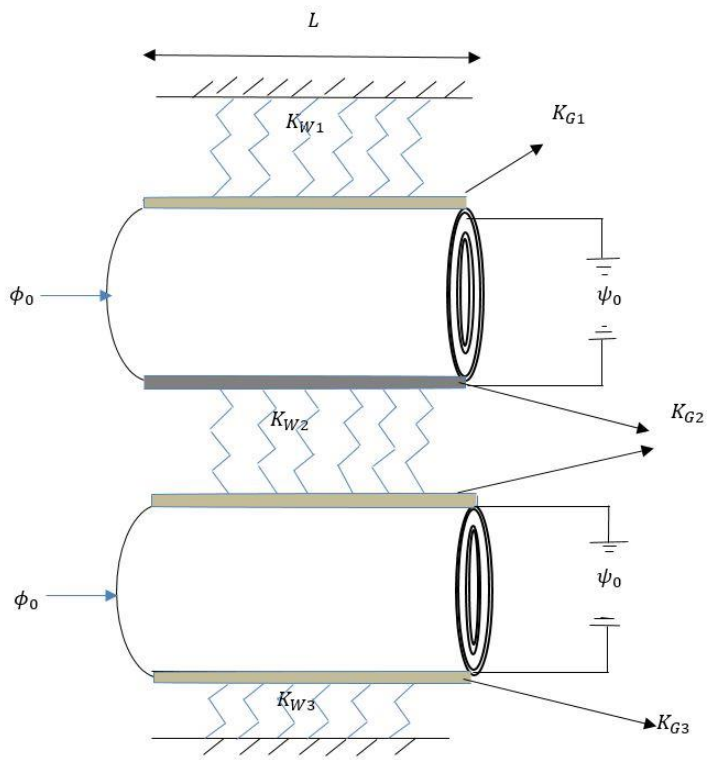

Fig. 1 A schematic view of double bonded micro-sandwich plate CNT/BNNT reinforced composite facesheets

2. Geometry and simulation

Fig. 1 illustrates a schematic view of double bonded micro sandwich cylindrical shell with saturated porous core and reinforced carbon nanotube piezoelectric composite face sheets. Length, thickness and inner radius of the micro sandwich cylindrical shell are L, h and R, respectively. h_c, h_b and h_t are the thicknesses of core, down and upper face sheets, respectively. The micro sandwich cylindrical shell with temperature dependent material properties is embedded by Pasternak foundation with K_{W_i} and K_{G_i}, $i = 1,2,3$. The micro sandwich cylindrical shell is subjected to applied voltage ψ_0 and magnetic field ϕ_0.

According to variation of porous distribution types along thickness, the following relations can be written as follows for core (Jabbari *et al*. 2013):

For porous nonlinear-nonsymmetric distribution

$$\begin{Bmatrix} G(z) \\ E(z) \\ \rho(z) \end{Bmatrix} = \begin{Bmatrix} G_0 \\ E_0 \\ \rho_0 \end{Bmatrix} \left[1 - e_1 \cos\left(\frac{\pi}{2h} \left(z + \frac{h}{2} \right) \right) \right], \tag{1a}$$

The initial shear modulus, Poisson's ratio and density are $G_0 = 24$ GPa, $\nu_0 = 0.3$ and $\rho_0 = 2700\ \mathrm{kg/m^3}$.

For porous-monotonous distribution

$$\begin{Bmatrix} G(z) \\ E(z) \\ \rho(z) \end{Bmatrix} = \begin{Bmatrix} G_0 \\ E_0 \\ \rho_0 \end{Bmatrix} \left[1 - e_1 \cos\left(\frac{\pi z}{h} \right) \right]. \tag{1b}$$

For porous-nonlinear-symmetric distribution

$$\begin{Bmatrix} G(z) \\ E(z) \\ \rho(z) \end{Bmatrix} = \begin{Bmatrix} G_0 \\ E_0 \\ \rho_0 \end{Bmatrix} (1 - e_1). \tag{1c}$$

The extended mixture approach is used for effective material properties of upper and lower face sheets as follows (Arani *et al*. 2016, Mohammadimehr *et al*. 2018a, b, c)

$$\begin{aligned} &E_{11} = \eta_1 V_{NT} E_{11}^{NT} + V_m E_m, \\ &\frac{\eta_2}{E_{22}} = \frac{V_{NT}}{E_{22}^{NT}} + \frac{V_m}{E_m}, \quad \frac{\eta_3}{G_{12}} = \frac{V_{NT}}{G_{12}^{NT}} + \frac{V_m}{G_m}, \end{aligned} \tag{2}$$

where $\eta_i\ (i = 1,2,3)$ are efficiency coefficients of nanotubes (NTs) including CNT and BNNT. These coefficients are listed in Table 1. E_{11}, E_{22} and $G_{12}$are the Young's modulii and the shear modulus of the NT, and $V_{NT}$and V_m are the volume fraction of the NT and the matrix, respectively. The material properties of SWCNTs and SWBNNTs for different temperatures are listed in Tables 2 and 3, respectively. Various distributions of NT are defined as

Table 1 Efficiency coefficients of NTs (Arani *et al*. 2016)

V_{NT}^*	η_1	η_2	η_3
0.11	0.149	0.934	0.934
0.14	0.150	0.941	0.941
0.17	0.149	1.381	1.381

Table 2 The temperature dependent material properties for (10, 10) SWCNT (R = 0.68 nm, L = 9.26 nm, h = 0.067 nm, $\rho = 1400\ Kg/m^3$, $\nu_{12} = 0.175$) (Farajpour *et al*. 2016)

Temperature (K)	$E_{11}^{CNT}(TPa)$	$E_{22}^{CNT}(TPa)$	$G_{12}^{CNT}(TPa)$	$\alpha_{11}^{CNT}(1/GPa.K)$	$\alpha_{22}^{CNT}(1/GPa.K)$
300	5.6466	7.08	1.9445	3.4584	5.1682
500	5.5308	6.9348	1.9643	4.5361	5.0189
700	5.4744	6.8641	1.9644	4.6677	4.8943

Table 3 The mechanical and electrical properties for CNT and BNNT as reinforced in face sheets (Ghorbanpour Arani *et al*. 2012, Mohammadimehr *et al*. 2016a, b)

All constants	The values of parameters
$Elasticconstants$ (CNT)	$C_{11} = 5.8249\,TPa,\quad C_{12} = 1.01937TPa,\quad C_{22} = 7.3037TPa$ $C_{44} = C_{55} = C_{66} = 1.9445TPa,\quad \upsilon = 0.175,\quad V_{CNT} = 0.17$
$Elasticconstants$ $(BNNTs)$	$C_{11} = C_{22} = C_{33} = 2.035\,TPa,\quad C_{12} = C_{13} = C_{23} = 0.692TPa,$ $C_{44} = C_{55} = C_{66} = 0.672TPa,\quad \upsilon = 0.34,\quad V_{NT} = 0.17$
$Piezoelectricconstants$ $(BNNT)$	$e_{31} = 0.95Cm^2,\quad e_{32} = -0.45Cm^2,$ $e_{24} = -0.273Cm^2,\quad e_{15} = -0.009C/m^2$
$Dielectricconstants$	$\mathrm{K}_{11} = \mathrm{K}_{22} = \mathrm{K}_{33} = 1.7708 \times 10^{-10}$

Table 4 The properties of matrix materials for face sheet layers ($BiTiO_3 - CoFe_2O_4$)

All constants	The values of parameters
$Elasticconstants$	$C_{11} = C_{22} = 226MPa,\quad C_{12} = 125MPa,\quad C_{13} = 124MPa,$ $C_{33} = 216MPa,\quad C_{44} = C_{55} = 44.2MPa,\quad C_{66} = 50.5MPa,$
$Piezoelectricconstants$	$e_{31} = e_{32} = -2.2Cm^2,\quad e_{15} = e_{24} = 5.8Cm^2,\quad e_{33} = 9.3Cm^2,$ $q_{31} = q_{32} = 290.1H/\mathrm{m},\quad q_{15} = q_{24} = 275H/\mathrm{m},\quad q_{33} = 349.9H/\mathrm{m},$
$Dielectricconstants$	$\mathrm{K}_{11} = \mathrm{K}_{22} = 5.64 \times 10^{-9}, \mathrm{K}_{33} = 6.35 \times 10^{-9},$
$Magnetoelectricconstants$	$g_{11} = g_{22} = 5.367 \times 10^{-12}V/m.Oe, g_{33} = 2737.5 \times 10^{-12}V/m.Oe,$
$Magneticconstants$	$\mu_{11} = \mu_{22} = -297 \times 10^{-6}N/A^2,\quad \mu_{33} = 53.5 \times 10^{-6}N/A^2,$
$Otherconstants$	$\rho = 5550kg/m^3,\quad \alpha = 4.74\mathrm{e}-5\quad 1/K,\quad \nu = 0.25,\quad \mathrm{h} = 2\mu\mathrm{m},$ $\mathrm{l} = 17.6\mu\mathrm{m},\quad \mathrm{L} = 20\mathrm{h},\quad \mathrm{K}_W = 600\mathrm{GN/m}^3,\quad \mathrm{K}_G = 1000\mathrm{N/m}$

$$V_{NT}(z) = \begin{cases} V_{NT}^*(UD - NT), \\ \left(1 + \dfrac{2z}{h}\right) V_{NT}^*(FG - V - NT), \\ 2\left(1 - \dfrac{|2z|}{h}\right) V_{NT}^*(FG - O - NT), \\ 2\dfrac{|2z|}{h} V_{NT}^*(FG - X - NT), \end{cases} \tag{3}$$

where

$$V_{NT}^* = \frac{w_{NT}}{w_{NT} + \left(\frac{\rho_{NT}}{\rho_m}\right)(1 - w_{NT})} \tag{4}$$

where w_{SWCNT} is the mass fraction of the nanotubes. ρ_{NT} and ρ_m are densities of NTs and the matrix, respectively. The properties of matrix materials for face sheet layers ($BiTiO_3$-$CoFe_2O_4$) is considered in Table 4.

Density, Poisson's ratio, thermal and hydro properties of face sheets are written as

$$\begin{aligned} \rho &= \rho_{NT}V_{NT} + \rho_m V_m, \\ \nu_{12} &= \nu_{12}^{NT}V_{NT} + \nu_m V_m, \\ \alpha_{11} &= \alpha_{11}^{NT}V_{NT} + \alpha_m V_m, \\ \alpha_{22} &= (1 + \nu_{12}^{NT})\alpha_{22}^{NT}V_{NT} + (1 + \nu_m)\alpha_m V_m - \nu_{12}\alpha_{11}, \\ \beta_{11} &= \beta_{11}^{NT}V_{NT} + \beta_m V_m, \\ \beta_{22} &= (1 + \nu_{12}^{NT})\beta_{22}^{NT}V_{NT} + (1 + \nu_m)\beta_m V_m - \nu_{12}\beta_{11}. \end{aligned} \tag{5}$$

The face sheets are reinforced by NTs. The volume fraction of NTs, V_{NT} for the top and the bottom of face sheets are as

$$\begin{aligned} V_{NT} &= 2\left(\frac{t_1 - z}{t_1 - t_0}\right)\overset{*}{V}_{NT}, \\ V_{NT} &= 2\left(\frac{z - t_2}{t_3 - t_2}\right)\overset{*}{V}_{NT}. \end{aligned} \tag{6}$$

Using Tables 3 and 4, the equal properties for face sheets can be obtained as follows (Zenkour 2015)

$$
\begin{aligned}
c_{11} &= \frac{c_{11}^{SWNT} c_{11}^{m}}{V_{SWNT} c_{11}^{m} + (1 - V_{SWNT}) c_{66}^{m}}, \\
c_{12} &= c_{11} \left[\frac{V_{SWNT} c_{12}^{SWNT}}{c_{11}^{SWNT}} + (1 - V_{SWNT}) \frac{c_{12}^{m}}{c_{11}^{m}} \right], \\
c_{22} &= V_{SWNT} c_{22}^{SWNT} + (1 - V_{SWNT}) c_{22}^{m}, \\
c_{66} &= \frac{c_{66}^{SWNT} c_{66}^{m}}{V_{SWNT} c_{66}^{SWNT} + (1 - V_{SWNT}) c_{66}^{m}},
\end{aligned} \tag{7a}
$$

$$
\begin{aligned}
e_{24} &= V_{SWNT} e_{24}^{SWNT} + (1 - V_{SWNT}) e_{24}^{m}, \\
e_{32} &= V_{SWNT} e_{32}^{SWNT} + (1 - V_{SWNT}) e_{32}^{m}, \\
e_{31} &= q_{11} \left(\frac{(1 - V_{SWNT}) e_{31}^{SWNT}}{q_{11}^{SWNT}} + \frac{V_{SWNT} e_{31}^{m}}{q_{11}^{m}} \right), \\
e_{15} &= \frac{e_{15}^{m} e_{15}^{SWNT}}{V_{SWNT} e_{15}^{m} + (1 - V_{SWNT}) e_{15}^{SWNT}},
\end{aligned} \tag{7b}
$$

$$
\begin{aligned}
K_{11} &= (1 - V_{SWNT}) K_{11}^{m} + V_{SWNT} K_{11}^{SWNT}, \\
K_{22} &= (1 - V_{SWNT}) K_{22}^{m} + V_{SWNT} K_{22}^{SWNT}, \\
K_{33} &= (1 - V_{SWNT}) K_{33}^{m} + V_{SWNT} K_{33}^{SWNT}.
\end{aligned} \tag{7c}
$$

Stiffness, piezoelectric and magnetic coefficients for face sheets can be stated in Appendix A. Displacement fields of the micro sandwich moderately cylindrical shell based on Cooper-Naghdi theory are given by

$$
\begin{aligned}
U_x(x,\theta,z,t) &= u(x,\theta,t) + z\beta_x(x,\theta,t), \\
U_\theta(x,\theta,z,t) &= v(x,\theta,t) + z\beta_\theta(x,\theta,t) \\
U_z(x,\theta,z,t) &= w(x,\theta,t),
\end{aligned} \tag{8}
$$

where $u(x,\theta,t)$, $v(x,\theta,t)$, $w(x,\theta,t)$, $\beta_x(x,\theta,t)$ and $\beta_\theta(x,\theta,t)$ are middle surface displacements and rotations in the longitudes, peripheral and thickness direction of the micro sandwich moderately cylindrical shell.

Strain-displacement relations for each of face sheet and core can be expressed as

$$
\begin{aligned}
\varepsilon_{xx} &= \frac{\partial U_x}{\partial x} = \frac{\partial u}{\partial x} + z\frac{\partial \beta_x}{\partial x}, \\
\varepsilon_{\theta\theta} &= \frac{U_z}{R} + \frac{1}{R}\frac{\partial U_\theta}{\partial \theta} = \frac{1}{R}\left(w + \frac{\partial v}{\partial \theta} + z\frac{\partial \beta_\theta}{\partial \theta} \right), \\
\varepsilon_{z\theta} &= \frac{1}{2}\left(\frac{1}{R}\frac{\partial U_z}{\partial \theta} + \frac{\partial U_\theta}{\partial z} - \frac{v}{R} \right) = \frac{1}{2}\left(\frac{1}{R}\frac{\partial w}{\partial \theta} + \beta_\theta - \frac{v}{R} \right), \\
\varepsilon_{xz} &= \frac{1}{2}\left(\frac{\partial U_z}{\partial x} + \frac{\partial U_x}{\partial z} \right) = \frac{1}{2}\left(\frac{\partial w}{\partial x} + \beta_x \right), \\
\varepsilon_{\theta x} &= \frac{1}{2}\left(\frac{1}{R}\frac{\partial U_x}{\partial \theta} + \frac{\partial U_\theta}{\partial x} \right). \\
&= \frac{1}{2}\left[\frac{1}{R}\left(\frac{\partial u}{\partial \theta} + z\frac{\partial \beta_x}{\partial \theta} \right) + \frac{\partial v}{\partial x} + z\frac{\partial \beta_\theta}{\partial x} \right]
\end{aligned} \tag{9}
$$

Hamilton's principle can be stated as follows

$$
\int_0^t (\delta T - \delta U - \delta W)\mathrm{d}t = 0, \tag{10}
$$

where δU,δW and$\delta T$are the variations of strain energy, work done by external force and kinetic energy, respectively. The variation of strain energy for three layers of the micro sandwich moderately cylindrical shell based on modified couple stress theory can be written as follows

$$
\begin{aligned}
\delta U = &\int_{-\frac{h_c}{2}-h_b}^{-\frac{h_c}{2}} \left(\sigma_{ij}\delta\varepsilon_{ij} + m_{ij}\delta\chi_{ij} - D_i\delta E_i - B_i\delta H_i \right) \mathrm{d}V \\
&+ \int_{-\frac{h_c}{2}}^{\frac{h_c}{2}} \left(\sigma_{ij}\delta\varepsilon_{ij} + m_{ij}\delta\chi_{ij} \right) \mathrm{d}V \\
&+ \int_{\frac{h_c}{2}}^{\frac{h_c}{2}+h_t} \left(\sigma_{ij}\delta\varepsilon_{ij} + m_{ij}\delta\chi_{ij} - D_i\delta E_i - B_i\delta H_i \right) \mathrm{d}V,
\end{aligned} \tag{11}
$$

where the stress tensor σ_{ij}, symmetric stress tensor m_{ij} and symmetric rotation gradient tensor are defined in Appendix B.

Electrical and magnetic potential functions can be expressed as (Farajpour *et al*. 2016)

$$
\begin{aligned}
\psi(x,\theta,z,t) &= \frac{2\tilde{z}}{h_p}\psi_0 - \psi(x,\theta,t)\cos\left(\frac{\pi\tilde{z}}{h_p} \right), \\
\varphi(x,\theta,z,t) &= \frac{2\tilde{z}}{h_p}\varphi_0 - \varphi(x,\theta,t)\cos\left(\frac{\pi\tilde{z}}{h_p} \right), \\
\tilde{z} &= z - \frac{h_c}{2} - \frac{h_t}{2}.
\end{aligned} \tag{12}
$$

Electric field E_i, magnetic field H_i, piezo-magnetic strain tensor B_i and dielectric displacement tensor D_i are defined in Appendix C.

The resultants forces and moments, some other parameters related to material length scale parameter, electric and magnetic fields are defined in Appendix D.

The variation of kinetic energy is given by

$$
\begin{aligned}
&\int_\Omega \delta T = \int_{-\frac{h_c}{2}-h_b}^{\frac{h_c}{2}+h_t} \delta T + \int_{-\frac{h_c}{2}-h_b}^{\frac{h_c}{2}+h_t} \delta T + \int_{\frac{h_c}{2}}^{\frac{h_c}{2}+h_t} \delta T, \\
&\delta T = \int_\Omega \rho(z) \begin{bmatrix} \frac{\partial U_x}{\partial t}\delta\left(\frac{\partial U_x}{\partial t}\right) \\ + \frac{\partial U_\theta}{\partial t}\delta\left(\frac{\partial U_\theta}{\partial t}\right) + \frac{\partial U_z}{\partial t}\delta\left(\frac{\partial U_z}{\partial t}\right) \end{bmatrix} \mathrm{d}V, \\
&\delta T = \\
&\int_\Omega \rho(z) \begin{bmatrix} \left(\frac{\partial u}{\partial t} + z\frac{\partial \beta_x}{\partial t}\right)\delta\left(\frac{\partial u}{\partial t} + z\frac{\partial \beta_x}{\partial t}\right) \\ + \left(\frac{\partial v}{\partial t} + z\frac{\partial \beta_\theta}{\partial t}\right)\delta\left(\frac{\partial v}{\partial t} + z\frac{\partial \beta_\theta}{\partial t}\right) \\ + \frac{\partial w}{\partial t}\delta\left(\frac{\partial w}{\partial t}\right) \end{bmatrix} \mathrm{d}x\mathrm{d}\theta\mathrm{d}z,
\end{aligned} \tag{13}
$$

Variation of kinetic energy must be extended for three layers of the micro sandwich cylindrical shell. Variation of work done by foundation forces for double bonded micro sandwich cylindrical shells can be written as follows (Mohammadimehr *et al*. 2016a, Mohammadimehr and Shahedi 2016)

$$
\delta W = \int_A F^{\mathrm{elastic}} \delta w \mathrm{d}A, \tag{14}
$$

$$\begin{aligned} F_1^{\text{elastic}} &= K_{W_1} w_1 - K_{W_2}(w_2 - w_1) \\ &\quad - K_{G_1}\nabla^2 w_1 + K_{G_2}\nabla^2(w_2 - w_1), \\ F_2^{\text{elastic}} &= K_{W_2}(w_2 - w_1) - K_{G_2}\nabla^2(w_2 - w_1) \\ &\quad + K_{W_3} w_2 - K_{G_3}\nabla^2 w_2. \end{aligned} \tag{14}$$

Employing Eqs. (12)-(14), the governing equations based on displacement are derived in Appendix E. Also, the coefficients of Eqs. (E-1) to (E-14) are addressed in Appendix F.

3. Solving method

Navier's solution is employed for simply supported boundary conditions of the micro sandwich cylindrical shell as follows

$$\begin{Bmatrix} \{u_i, \beta_{x_i}, \beta_{t_i}\} \\ v_i \\ \{w_i, \varphi_i, \psi_i\} \end{Bmatrix}(x,\theta,t) = \sum_{m=1}^{\infty}\sum_{n=1}^{\infty} \begin{Bmatrix} \{U_{mni}, \beta_{x_{mni}}, \beta_{t_{mni}}\}\cos\left(\frac{m\pi x}{L}\right)\cos(n\theta) \\ V_{mni}\sin\left(\frac{m\pi x}{L}\right)\sin(n\theta) \\ \{W_{mni}, \varphi_{mni}, \psi_{mni}\}\sin\left(\frac{m\pi x}{L}\right)\cos(n\theta) \end{Bmatrix} e^{j\omega} \tag{15}$$

where $i = 1,\ 2$, m and n are half axial and peripheral wave numbers, respectively. In the matrix form (Mohammadimehr and Rahmati 2013)

$$\{[K] - [M]\omega_{mn}^2\}\{U\} = 0, \tag{16}$$

where $[K]$, $[M]$ and $\{U\}$ are stiffness matrix, mass matrix and displacement vector, respectively.

4. Numerical result and discussion

In order to ensure the obtained results from the free vibration analysis of Cooper-Naghdi micro sandwichcylindrical shells with saturated porous core and reinforced carbon nanotube piezoelectric composite face sheets, theresults are compared with other researches (Loy *et al*. 1997, Wang and Wu 2017, Ke *et al*. 2015) in Tables 5-6 that the dimensionless natural frequencies of micro composite sandwich cylindrical shells ($\overline{\omega} = \omega R\sqrt{\rho(1-\nu_{12}^2)/E_{11}}$). The dimensionless natural frequencies of piezoelectric andporous cylindrical nanoshells are reported in Tables 5 and 6, respectively. The obtained results have a good agreement with the literature.

The influence of various factors such as the SWNT volume fraction, length to thickness ratio, temperature change, porosity distribution, small scale coefficient, theface sheet thickness to the core thickness ratio, foundation constants on the natural frequency of double-

Table 5 The dimensionless natural frequencies of piezoelectric cylindrical nanoshells

n	Present work	Ke *et al*. (2015)	Error (%)	Loy *et al*. (1997)	Error (%)
1	0.0158	0.0168	1.37	0.0161	1.4
2	0.00936	0.00938	0.2	0.00938	0.2
3	0.02209	0.02210	0.08	0.02210	0.06
4	0.04206	0.04209	0.09	0.04209	0.08

Table 6 The dimensionless natural frequencies of porous cylindrical nanoshells with uniform distribution

n	Present work	Wang and Wu (2017)	Error (%)
1	0.0168	0.0161	4.3
2	0.0096	0.0094	2.12
3	0.0222	0.0221	0.45
4	0.0423	0.0421	0.47
5	0.0683	0.0680	0.44

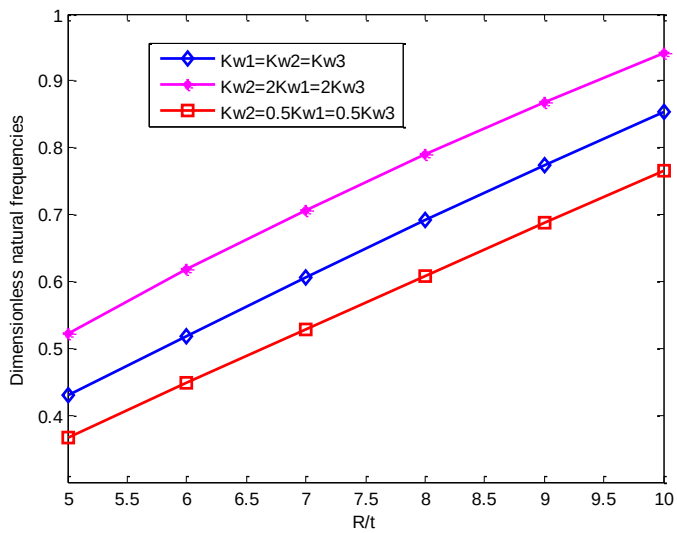

Fig. 2 The dimensionless natural frequencies of double-bonded micro sandwich cylindrical shell versus radius to thickness ratio for various spring constants

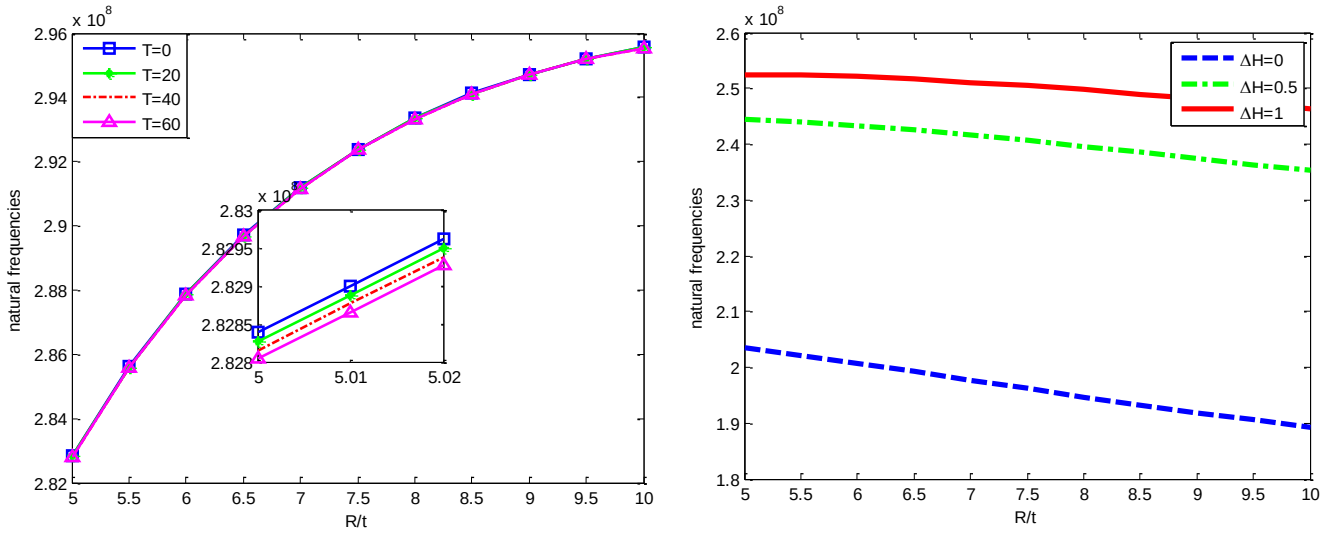

(a) (b)

Fig. 3 The naturhpgal frequencies of double-bonded micro sandwich cylindrical shell versus radius to thickness ratio for various (a) temperature change; (b) moisture change

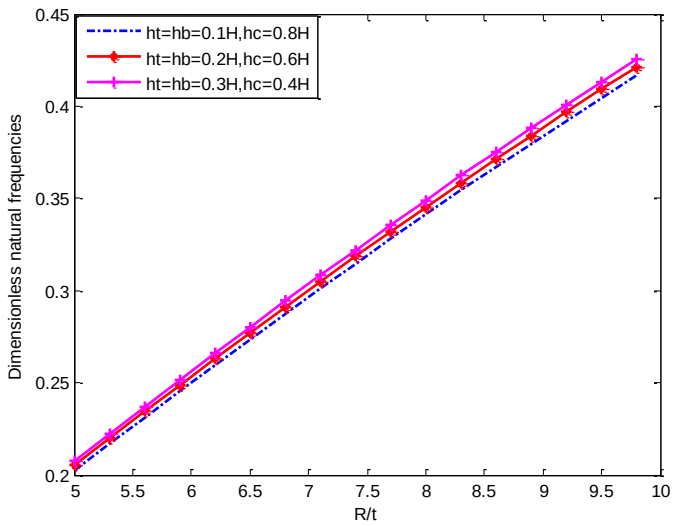

Fig. 4 The dimensionless natural frequencies of double-bonded micro sandwich cylindrical shells versus radius to thickness ratio for various thicknesses of facesheets and cores

bonded micro sandwich cylindrical shells with saturated porous core andCNT/BNNT reinforced composite face sheets under hydro-thermo-mechanical loadings based on Cooper-Naghdi theory are studied.

Fig. 2 depicts the dimensionless natural frequencies of double-bonded micro sandwich cylindrical shell with saturated porous core and carbon nanotube reinforced piezoelectric composite face sheets for radius to thickness ratio (R/t). As the figure shows, with increasing the radius to thickness ratio of double-bonded micro sandwich cylindrical shell, the dimensionless natural frequency increases. Also, it can be seen that by increasing the spring constants between two micro shells, the dimensionless natural frequencies enhances. It is due to increasing the stiffness of micro structure.

The effect of temperature and moisture changes on the natural frequencies of the double-bonded micro sandwich cylindrical shell is shown in Figs. 3(a) and (b), respectively. It can be seen that as the temperature rises, the natural frequency and the stiffness of the micro sandwich cylindrical shell decreases; while this note is vice versa for moisture changes.

Fig. 4 illustrates the dimensionless natural frequencies of double-bonded micro sandwich cylindrical shell versus radius to thickness ratio for various thicknesses offacesheets and cores. It can be seen that with increasing thickness of face sheets, the dimensionless natural frequency increases due to enhancing the stiffness of doublebonded micro sandwich shells.

Fig. 5 shows the effect of volume fraction of SWCNTs on the dimensionless natural frequency. It is expected that with adding SWCNTs to double-bonded micro sandwich

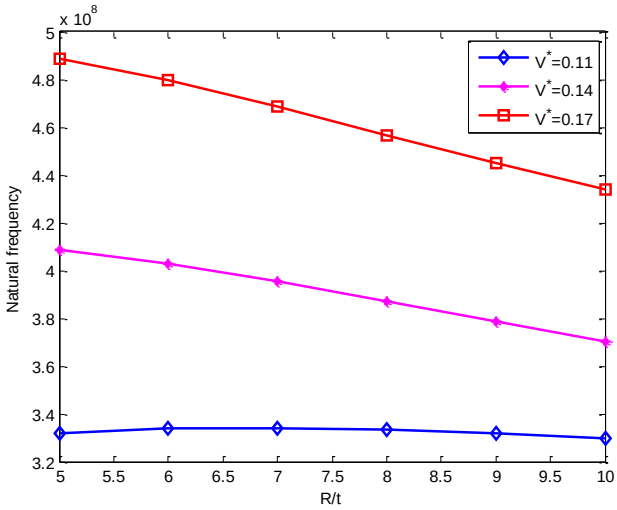

Fig. 5 Influence of SWCNT volume fraction on the dimensionless natural frequencies of double-bhpgonded micro sandwich cylindrical shells

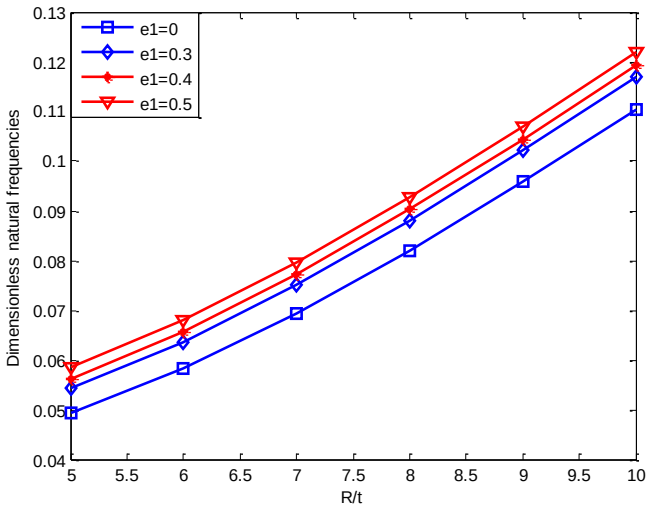

Fig. 6 Influence of porosity coefficient on the dimensionless natural frequencies of double-bonded micro sandwich cylindrical shells

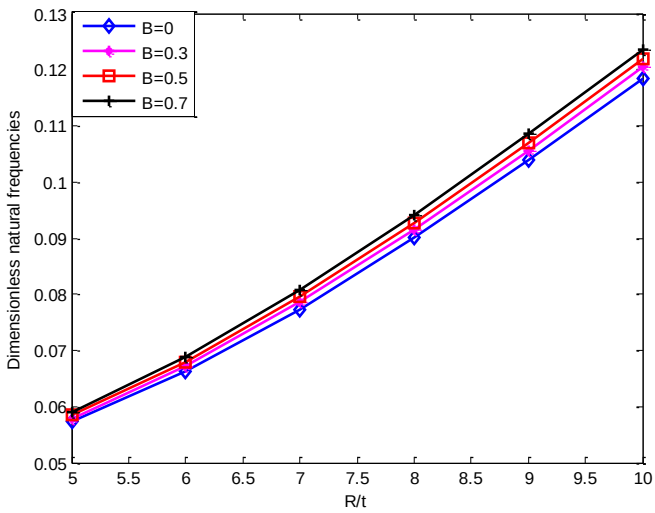

Fig. 7 Influence of porosity coefficient on the dimensionless natural frequencies of double-bonded micro sandwich cylindrical shells

cylindrical shells, the stiffness of the structure increases, which leads to enhance the dimensionless natural frequency.

In the Fig. 6, by increasing the porosity coefficient and radius to thickness ratio, the natural frequency of double bonded micro sandwich cylindrical shells increases and thisincrease is more in the higher porosity coefficient. As the porosity increases, the free space volume of double bonded micro sandwich cylindrical shells enhances, and the weight of the structure decreases, as well as its stiffness. But the effect of the structure's stiffness is higher, so dimensionless natural frequency of double bonded micro sandwich cylindrical shells increases with increasing porosity.

5. Conclusions

In this research, based on Cooper-Naghdi theory, free vibration analysis of double bonded micro sandwich cylindrical shells with saturated porous core and carbon/ boron nitride nanotubes (CNT/BNNT) reinforced composite face sheets subjected to hydro-thermo-mechanical loadings is presented. The material properties of the structure are assumed to be temperature dependent, and each of the micro-tubes is placed on the Pasternak elastic foundations, and mechanical, moisture, thermal, electrical, and magnetic forces are effective on the structural behavior. The distribution of porous materials in three distributions such as non-linear non-symmetric porosity, nonlinear-symmetric of porosity, and uniform porosity are considered. The relationship including electro-magneto-hydro-thermo-mechanical loadings based on modified couple stress theory is obtained. Also by using the energy method and the Hamilton's principle, the governing equations of motion are derived. In this article, the effects of various parameters such as material length scale parameter, temperature change, distributions of nanotube, volume fraction of nanotubes, porosity and Skempton coefficients, and geometric parameters on the natural frequency are investigated. Also, in order to ensure the obtained results from the free vibration analysis of Cooper-Naghdi micro sandwich cylindrical shells with saturated porous core and reinforced carbon nanotube piezoelectric composite face sheets, the results are compared with other researches that have a good agreement with the literature results. It can be seen that with increasing of radius to the thickness ratio of double-bonded micro sandwich cylindrical shell, the dimensionless natural frequency of the system increases. Also, it can be seen that by increasing the spring constants between two micro shells, the dimensionless natural frequencies enhances. It is due to increasing the stiffness of micro structure. It can be seen that as the temperature rises, the natural frequency and the stiffness of the micro sandwich cylindrical shell decreases; while this note is vice versa for moisture changes. Moreover, with increasing thickness of face sheets, the dimensionless natural frequency increases due to enhancing the stiffness of double bonded micro sandwich shells.

Also, the natural frequency of double bonded micro sandwich cylindrical shells increases by increasing the porosity and Skempton coefficients and radius to thickness ratio, and this increase is more in the higher porosity coefficient. As the porosity increases, the free space volume of double bonded micro sandwich cylindrical shells enhances, and the weight of the structure decreases, as well as its stiffness. But the effect of the structure's stiffness is higher, so dimensionless natural frequency of double bonded micro sandwich cylindrical shells increases with increasing porosity.

Acknowledgments

The authors would like to thank the referees for their valuable comments. Also, they are thankful to thankthe Iranian Nanotechnology Development Committee for their financial support and the University of Kashan for supporting this work by Grant No. 682561/22.

References

Alashti, R.A. and Khorsand, M. (2012), "Three-dimensional dynamo-thermo-elastic of a functionally graded cylindrical shell with piezoelectric layers by DQ-FD coupled", *Int. J. Press. Vessels Pip.*, **96**, 49-67. https://doi.org/10.1016/j.ijpvp.2012.06.006

Arani, A.G., Mohammadimehr, M., Saidi, A.R., Shogaei, S. and Arefmanesh, A. (2011), "Thermal buckling analysis of double-walled carbon nanotubes considering the small-scale length effect", *Proc. IMechE, PartC, Journal of Mechanical Engineering Science*, **225**, 248-256. https://doi.org/10.1177/09544062JMES1975

Arani, A.G., Mobarakeh, M.R., Shams, S. and Mohammadimehr, M. (2012), "The effect of CNT volume fraction on the magneto-thermo-electro-mechanical behavior of smart nanocomposite cylinder", *J. Mech. Sci. Technol.*, **26**(8), 2565-2572. https://doi.org/10.1007/s12206-012-0639-5

Arani, A.G., Haghparast, E., Maraghi, Z.K. and Amir, S. (2015), "Static stress analysis of carbon nano-tube reinforced composite (CNTRC) cylinder under non-axisymmetric thermo-mechanical loads and uniform electro-magnetic fields", *Compos. Part B*, **68**, 136-145. https://doi.org/10.1016/j.compositesb.2014.08.036

Arani, A.G., Arani, H.K. and Maraghi, Z.K. (2016), "Vibration analysis of sandwich composite micro-plate under electro-magneto-mechanical loadings", *Appl. Math. Model.*, **40**, 10596-10615. https://doi.org/10.1016/j.apm.2016.07.033

Bahadori, R. and Najafizadeh, M.M. (2015), "Free vibration of two-dimensional functionally graded axisymmetric cylindrical shell on Winkler-Pasternak elastic foundation by first-order shear deformation theory and using Navier differential quadrature solution methods", *Appl. Math. Model.*, **39**, 4877-4894. https://doi.org/10.1016/j.apm.2015.04.012

Barati, M.R. and Zenkour, A. (2017), "A general bi-Helmholtz nonlocal strain-gradient elasticity for wave propagation in nanoporous graded double-nanobeam systems on elastic substrate", *Compos. Struct.*, **168**, 885-892. https://doi.org/10.1016/j.compstruct.2017.02.090

Barati, M.R. and Zenkour, A.M. (2018), "Electro-thermoelastic vibration of plates made of porous functionally graded piezoelectric materials under various boundary conditions", *J. Vib. Control*, **24**(10), 1910-1926. https://doi.org/10.1177/1077546316672788

Barati, M.R., Sadr, M.H. and Zenkour, A.M. (2016), "Buckling

analysis of higher order graded smart piezoelectric plates with porosities resting on elastic foundation", *Int. J. Mech. Sci.*, **117**, 309-320. https://doi.org/10.1016/j.ijmecsci.2016.09.012

Barati, M.R., Shahverdi, H. and Zenkour, A.M. (2017), "Electro-mechanical vibration of smart piezoelectric FG plates with porosities according to a refined four-variable theory", *Mech. Adv. Mater. Struct.*, **24**(12), 987-998. https://doi.org/10.1080/15376494.2016.1196799

Beni, Y.T., Mehralian, F. and Razavi, H. (2015), "Free vibration analysis of size-dependent shear deformation functionally graded cylindrical shell on the basis of modified couple stress theory", *Compos. Struct.*, **120**, 65-78. https://doi.org/10.1016/j.compstruct.2014.09.065

Dey, T. and Ramachandra, L.S. (2016), "Non-linear vibration analysis of laminated composite circular cylindrical shells", *Compos. Struct.*, **163**, 89-100. https://doi.org/10.1016/j.compstruct.2016.12.018

Do, Q.C., Pham, D.N., Vu, D.Q., Vu, T.T.A. and Nguyen, D.D. (2019), "Nonlinear buckling and post-buckling of functionally graded carbon nanotubes reinforced composite truncated conical shells subjected to axial load", *Steel Compos. Struct., Int. J.*, **31**(3), 243-259. https://doi.org/10.12989/scs.2019.31.3.243

Duc, N.D. (2014), "Nonlinear static and dynamic stability of functionally graded plates and shells", Vietnam National University Press, Hanoi, Vietnam.

Duc, N.D., Cong, P.H., Anh, V.M., Quang, V.D., Tran, P., Tuan, N.D. and Thinh, N.H. (2015a), "Mechanical and thermal stability of eccentrically stiffened functionally graded conical shell panels resting on elastic foundations and in thermal environment", *Compos. Struct.*, **132**, 597-609. https://doi.org/10.1016/j.compstruct.2015.05.072

Duc, N.D., Tuan, N.D., Tran, P., Dao, N.T. and Dat, N.T. (2015b), "Nonlinear dynamic analysis of Sigmoid functionally graded circular cylindrical shells on elastic foundations using the third order shear deformation theory in thermal environments", *Int. J. Mech. Sci.*, **101-102**, 338-348. https://doi.org/10.1016/j.ijmecsci.2015.08.018

Duc, N.D., Bich, D.H. and Cong, P.H. (2016), "Nonlinear thermal dynamic response of shear deformable FGM plates on elastic foundations", *J. Thermal Stress.*, **39**(3), 278-297.

Duc, N.D., Lee, J., Nguyen-Thoi, T. and Thang, P.T. (2017), "Static response and free vibration of functionally graded carbon nanotube-reinforced composite rectangular plates resting on Winkler-Pasternak elastic foundations", *J. Aerosp. Sci. Technol.*, **68**, 391-402. https://doi.org/10.1016/j.ast.2017.05.032

Farajpour, A., Yazdi, M.H., Rastgoo, A., Loghmani, M. and Mohammadi, M. (2016), "Nonlocal nonlinear plate model for large amplitude vibrationof magneto-electro-elastic nanoplate", *Compos. Struct.*, **140**, 323-336. https://doi.org/10.1016/j.compstruct.2015.12.039

Frostig, Y., Birman, V. and Kardomateas, G.A. (2018), "Non-linear wrinkling of a sandwich panel with functionally graded core – Extended high-order approach", *Int. J. Solids Struct.*, **148-149**, 122-139. https://doi.org/10.1016/j.ijsolstr.2018.02.023

Ghorbanpour Arani, A., Amir, S., Shajari, A.R., Mozdianfard, M.R., Khoddami Maraghi, Z. and Mohammadimehr, M. (2012a), "Electro-thermal non-local vibration analysis of embedded DWBNNTs", *Proc. IMechE, PartC: Journal of Mechanical Engineering Science*, **226**, 1410-1422. https://doi.org/10.1177/0954406211422619

Ghorbanpour Arani, A., Rabbani, H., Amir, S., Khoddami Maraghi, Z., Mohammadimehr, M. and Haghparast, E. (2012b), "Analysis of nonlinear vibrations for multi-walled carbon nanotubes embedded in an elastic medium", *J. Solid Mech.*, **3**(3), 258-270.

Jabbari, M., Joubaneh, E.F., Khorshidvand, A.R. and Eslami, M.R. (2013), "Buckling analysis of porous circular plate with piezoelectric actuator layers under uniform radial compression", *Int. J. Mech. Sci.*, **70**, 50-56. https://doi.org/10.1016/j.ijmecsci.2013.01.031

Ke, L.L., Liu, C. and Wang, Y.S. (2015), "Free vibration of nonlocal piezoelectric nanoplates under various boundary conditions", *Physica E*, **66**, 93-106. https://doi.org/10.1016/j.physe.2014.10.002

Kheibari, F. and Beni, Y.T. (2016), "Size dependent electro-mechanical vibration of single-walled piezoelectricnanotubes using thin shell model", *Mater. Des.*, **114**, 572-583. https://doi.org/10.1016/j.matdes.2016.10.041

Khoa, N.D., Thiem, H.T. and Duc, N.D. (2019), "Nonlinear buckling and postbuckling of imperfect piezoelectric S-FGM circular cylindrical shells with metal-ceramic-metal layers in thermal environment using Reddy's third-order shear deformation shell theory", *Mech. Adv. Mater. Struct.*, **26**(3), 248-259. https://doi.org/10.1080/15376494.2017.1341583

Lei, Z.X., Zhang, L.W. and Liew, K.M. (2015), "Vibration analysis of CNT-reinforced functionally graded rotating cylindrical panels using the element-free kp-Ritz method", *Compos. Part B*, **77**, 291-303. https://doi.org/10.1016/j.compositesb.2015.03.045

Liu, S., Yu, T. and Bui, T.Q. (2017a) "Size effects of functionally graded moderately thick microplates: A novel non-classical simple-FSDT isogeometricanalysis", *Eur. J. Mech. - A/Solids*, **66**, 446-458. https://doi.org/10.1016/j.euromechsol.2017.08.008

Liu, S., Yu, T., Bui, T.Q. and Xia, S. (2017b), "Size-dependent analysis of homogeneous and functionally graded microplates using IGA and a non-classical Kirchhoff plate theory", *Compos. Struct.*, **172**, 34-44. https://doi.org/10.1016/j.compstruct.2017.03.067

Liu, S., Yu, T., Van Lich, L., Yin, S. and Bui, T.Q. (2018), "Size effect on cracked functional composite micro-plates by an XIGA-based effective approach", *Meccanica*, **53**(10), 2637-2658. https://doi.org/10.1007/s11012-018-0848-9

Liu, S., Yu, T., Van Lich, L., Yin, S. and Bui, T.Q. (2019), "Size and surface effects on mechanical behavior of thin nanoplates incorporating microstructures using isogeometric analysis", *Comput. Struct.*, **212**, 173-187. https://doi.org/10.1016/j.compstruc.2018.10.009

Loy, C.T., Lam, K.Y. and Shu, C. (1997), "Analysis of cylindrical shells using generalized differential quadrature", *Shock Vib.*, **4**, 193-198. https://doi.org/10.3233/SAV-1997-4305

Mehar, K., Panda, S.K., Bui, T.Q. and Mahapatra, T.R. (2017), "Nonlinear thermoelastic frequency analysis of functionally graded CNT-reinforced single/doubly curved shallow shell panels by FEM", *J. Thermal Stress.*, **40**, 899-916. https://doi.org/10.1080/01495739.2017.1318689

Minh, P.P. and Duc, N.D. (2019), "The effect of cracks on the stability of the functionally graded plates with variable-thickness using HSDT and phase-field theory", *Compos. Part B*, **175**, 107086. https://doi.org/10.1016/j.compositesb.2019.107086

Mohammadimehr, M. and Mehrabi, M. (2017), "Stability and free vibration analysis of double-bonded micro composite sandwich cylindrical shells conveying fluid flow", *Appl. Math Model*, **47**, 685-709. https://doi.org/10.1016/j.apm.2017.03.054

Mohammadimehr, M. and Rahmati, A.H. (2013), "Small scale effect on electro-thermo-mechanical vibration analysis of single-walled boron nitride nanorods under electric excitation", *Turkish J. Eng. Environ. Sci.*, **37**, 1-15.

Mohammadimehr, M. and Shahedi, S. (2016), "Nonlinear magneto-electro-mechanical vibration analysis of double-bonded sandwich Timoshenko microbeams based on MSGT using GDQM", *Steel Compos. Struct., Int. J.*, **21**(1), 1-36. https://doi.org/10.12989/scs.2016.21.1.001

Mohammadimehr, M., Saidi, A.R., Ghorbanpour Arani, A.,

Arefmanesh, A. and Han, Q. (2011), "Buckling analysis of double-walled carbon nanotubes embedded in an elastic medium under axial compression using non-local Timoshenko beam theory", *Proc. IMechE, Part C: Journal of Mechanical Engineering Science*, **225**(2), 498-506. https://doi.org/10.1177/2041298310392861

Mohammadimehr, M., Navi, B.R. and Arani, A.G. (2016a), "Modified strain gradient Reddy rectangular plate model for biaxialbuckling and bending analysis of double-coupled piezoelectricpolymeric nanocomposite reinforced by FG-SWNT", *Compos. Part B*, **87**, 132-148. https://doi.org/10.1016/j.compositesb.2015.10.007

Mohammadimehr, M., Salemi, M. and Navi, B.R. (2016b), "Bending buckling and free vibration analysis of MSGT microcomposite Reddy plate reinforced by FG-SWCNTs with temprature-dependent material properties under hydro-thermo-mechanical loadings using DQM", *Compos. Struct.*, **138**, 361-380.https://doi.org/10.1016/j.compstruct.2015.11.055

Mohammadimehr, M., Nejad, E.S. and Mehrabi, M. (2018a), "Buckling and vibration analyses of MGSGT double-bonded micro composite sandwich SSDT plates reinforced by CNTs and BNNTs with isotropic foam & flexible transversely orthotropic cores", *Struct. Eng. Mech., Int. J.*, **65**(4), 491-504. https://doi.org/10.12989/sem.2018.65.4.491

Mohammadimehr, M., Mohammadi-Dehabadi, A.A., Akhavan Alavi, S.M., Alambeigi, K., Bamdad, M., Yazdani, R. and Hanifehlou, S. (2018b), "Bending, buckling, and free vibration analyses of carbon nanotube reinforced composite beams and experimental tensile test to obtain the mechanical properties of nanocomposite", *Steel Compos. Struct., Int. J.*, **29**(3), 405-422 https://doi.org/10.12989/scs.2018.29.3.405

Mohammadimehr, M., Mehrabi, M., Hadizadeh, H. and Hadizadeh, H. (2018c), "Surface and size dependent effects on static, buckling, and vibration of micro composite beam under thermo-magnetic fields based on strain gradient theory", *Steel Compos. Struct., Int. J.*, **26**(4), 513-531. https://doi.org/10.12989/scs.2018.26.4.513

Murmu, T., McCarthy, M.A. and Adhikari, S. (2012), "Vibration response of double-walled carbon nanotubes subjected to an externally applied longitudinal magnetic field: A nonlocal elasticity approach", *J. Sound Vib.*, **331**, 5069-5086. https://doi.org/10.1016/j.jsv.2012.06.005

Nguyen, D.D. (2016), "Nonlinear thermo-electro-mechanical dynamic response of shear deformable piezoelectric Sigmoid functionally graded sandwich circular cylindrical shells on elastic foundations", *J. Sandw. Struct. Mater.*, 1-28. https://doi.org/10.1177/1099636216653266

Nguyen, D.K., Vu, M.A. and Nguyen, D.D. (2019b), "Nonlinear dynamic response and vibration of functionally graded nanocomposite cylindrical panel reinforced by carbon nanotubes in thermal environment", *J. Sandw. Struct. Mater.* https://doi.org/10.1177/1099636219847191

Pourasghar, A. and Chen, Z. (2016), "Thermoelastic response of CNT reinforced cylindrical panel resting on elastic foundation using theory of elasticity", *Compos. Part B: Eng.*, **99**, 436-444**.** https://doi.org/10.1016/j.compositesb.2016.06.028

Razavi, H., Babadi, A.F. and Beni, Y.T. (2016), "Free vibration analysis of functionally graded piezoelectric cylindrical nanoshell based on consistent couple stress theory", *Compos. Struct.*, **160**, 1299-1309. https://doi.org/10.1016/j.compstruct.2016.10.056

Shen, H.S., Xiang, Y., Fan, Y. and Hui, D. (2018), "Nonlinear vibration of functionally graded graphene-reinforced composite laminated cylindrical panels resting on elastic foundations in thermal environments", *Compos. Part B*, **136**, 177-186. https://doi.org/10.1016/j.compositesb.2017.10.032

Sobhy, M. and Zenkour, A.M. (2018), "Magnetic field effect on thermomechanical buckling and vibration of viscoelastic sandwich nanobeams with CNT reinforced face sheets on a viscoelastic substrate", *Compos. Part B: Eng.*, **154**, 492-506. https://doi.org/10.1016/j.compositesb.2018.09.011

Song, Z.G., Zhang, L.W. and Liew, K.M. (2016), "Vibration analysis of CNT-reinforced functionally graded composite cylindrical shells in thermal environments", *Int. J. Mech. Sci.*, **115**, 339-347. https://doi.org/10.1016/j.ijmecsci.2016.06.020

Van Do, T., Nguyen, D.K., Duc, N.D., Doan, D.H. and Bui, T.Q. (2017), "Analysis of bi-directional functionally graded plates by FEM and a new third-order shear deformation plate theory", *Thin-Wall. Struct.*, **119**, 687-699. https://doi.org/10.1016/j.tws.2017.07.022

Vuong, P.M. and Duc, N.D. (2018), "Nonlinear response and buckling analysis of eccentrically stiffened FGM toroidal shell segments in thermal environment", *J. Aerosp. Sci. Technol.*, **79**, 383-398. https://doi.org/10.1016/j.ast.2018.05.058

Wang, Y. and Wu, D. (2017), "Free vibration of functionally graded porous cylindrical shell using a sinusoidal shear deformation theory", *Aero. Sci. Technol.*, **66**, 83-91. https://doi.org/10.1016/j.ast.2017.03.003

Yang, J., Xiong, J., Ma, L., Zhang, G., Wang, X. and Wu, L. (2014), "Study on vibration damping of composite sandwich cylindrical shell with pyramidal truss-like cores", *Compos. Struct.*, **117**, 362-372. https://doi.org/10.1016/j.compstruct.2014.06.042

Yu, T., Zhang, J., Hu, H. and Bui, T.Q. (2019a), "A novel size-dependent quasi-3D isogeometric beam model for two-directional FG microbeams analysis", *Compos. Struct.*, **211**, 76-88. https://doi.org/10.1016/j.compstruct.2018.12.014

Yu, T., Hu, H., Zhang, J. and Bui, T.Q. (2019b), "Isogeometric analysis of size-dependent effects for functionally graded microbeams by a non-classical quasi-3D theory", *Thin-Wall. Struct.*, **138**, 1-14. https://doi.org/10.1016/j.tws.2018.12.006

Yuan, Z. and Kardomateas, G.A. (2018), "Nonlinear dynamic response of sandwich wide panels", *Int. J. Solids Struct.*, **148-149**, 110-121. https://doi.org/10.1016/j.ijsolstr.2017.09.028

Zeighampour, H. and Beni, Y.T. (2014), "Cylindrical thin-shell model based on modified strain gradient theory", *Int. J. Eng. Sci.*, **78**, 27-47. https://doi.org/10.1016/j.ijengsci.2014.01.004

Zenkour, A.M. (2015), "A comprehensive analysis of functionally graded sandwich plates: Part 2—Buckling and free vibration", *Int. J. Solids Struct.*, **42**, 5243-5258. https://doi.org/10.1016/j.ijsolstr.2005.02.016

Zenkour, A.M. (2018), "A quasi-3D refined theory for functionally graded single-layered and sandwich plates with porosities", *Compos. Struct.*, **201**, 38-48. https://doi.org/10.1016/j.compstruct.2018.05.147

CC

Appendix A

Stiffness, piezoelectric and magnetic coefficients for face sheets can be stated as the following form

$$Q_{11}(z) = \frac{E_{11}(z)}{1 - \upsilon_{12}(z)\upsilon_{21}(z)},$$

$$e_{24} = V_{SWNT} e_{24}^{SWNT} + (1 - V_{SWNT}) e_{24}^{m},$$

$$Q_{22}(z) = \frac{E_{22}(z)}{1 - \upsilon_{12}(z)\upsilon_{21}(z)},$$

$$e_{32} = V_{SWNT} e_{32}^{SWNT} + (1 - V_{SWNT}) e_{32}^{m},$$

$$Q_{12}(z) = \frac{\upsilon_{21}(z) E_{11}(z)}{1 - \upsilon_{12}(z)\upsilon_{21}(z)},$$

$$e_{31} = q_{11}\left(\frac{(1 - V_{SWNT}) e_{31}^{SWNT}}{q_{11}^{SWNT}} + \frac{V_{SWNT} e_{31}^{m}}{q_{11}^{m}}\right),$$

$$Q_{44}(z) = \frac{E_{22}(z)}{2\big(1 + \upsilon_{23}(z)\big)},$$

$$e_{15} = \frac{e_{15}^{m} e_{15}^{SWNT}}{V_{SWNT} e_{15}^{m} + (1 - V_{SWNT}) e_{15}^{SWNT}},$$

$$Q_{55}(z) = Q_{66}(z) = G_{12}(z),$$

$$\eta_{11} = (1 - V_{SWNT})\eta_{11}^{m} + V_{SWNT}\eta_{11}^{SWNT},$$

$$\eta_{22} = (1 - V_{SWNT})\eta_{22}^{m} + V_{SWNT}\eta_{22}^{SWNT},$$

$$\eta_{33} = (1 - V_{SWNT})\eta_{33}^{m} + V_{SWNT}\eta_{33}^{SWNT}.$$

Appendix B

The stress tensorσ_{ij}, symmetric stress tensor m_{ij} and symmetric rotation gradient tensor are defined as follows

$$\begin{Bmatrix} \sigma_{xx} \\ \sigma_{\theta\theta} \\ \sigma_{z\theta} \\ \sigma_{zx} \\ \sigma_{x\theta} \end{Bmatrix} = \begin{bmatrix} Q_{11} & Q_{12} & 0 & 0 & 0 \\ Q_{12} & Q_{22} & 0 & 0 & 0 \\ 0 & 0 & k_s Q_{44} & 0 & 0 \\ 0 & 0 & 0 & k_s Q_{55} & 0 \\ 0 & 0 & 0 & 0 & Q_{66} \end{bmatrix} \begin{Bmatrix} \varepsilon_{xx} - \alpha_{11}\Delta T \\ \varepsilon_{\theta\theta} - \alpha_{22}\Delta T \\ \gamma_{z\theta} \\ \gamma_{zx} \\ \gamma_{x\theta} \end{Bmatrix}$$

$$- \begin{bmatrix} 0 & 0 & e_{31} \\ 0 & 0 & e_{32} \\ 0 & e_{24} & 0 \\ e_{15} & 0 & 0 \\ 0 & 0 & 0 \end{bmatrix} \begin{Bmatrix} E_x \\ E_\theta \\ E_z \end{Bmatrix} - \begin{bmatrix} 0 & 0 & q_{31} \\ 0 & 0 & q_{32} \\ 0 & q_{24} & 0 \\ q_{15} & 0 & 0 \\ 0 & 0 & 0 \end{bmatrix} \begin{Bmatrix} H_x \\ H_\theta \\ H_z \end{Bmatrix},$$

$$m_{ij} = 2l^2 \mu \chi_{ij}, \quad \theta_i = \frac{1}{2}\mathrm{curl}(u), \quad \chi_{ij} = \frac{1}{2}\big(\theta_{i,j} + \theta_{\mathrm{j,i}}\big),$$

$$\chi_{xx} = \frac{1}{2}\left(\frac{1}{R}\frac{\partial^2 w}{\partial x\,\partial\theta} - \frac{1}{R}\frac{\partial v}{\partial x} - \frac{\partial \beta_\theta}{\partial x}\right),$$

$$\chi_{\theta\theta} = \frac{1}{2R}\left(\frac{\partial v}{\partial x} - \frac{1}{R}\frac{\partial u}{\partial \theta} - \frac{\partial^2 w}{\partial x\,\partial\theta} + \frac{\partial \beta_x}{\partial \theta} + z\frac{\partial \beta_\theta}{\partial x}\right),$$

$$\chi_{zz} = \frac{1}{2}\left(\frac{1}{R^2}\frac{\partial u}{\partial \theta} - \frac{1}{R}\frac{\partial \beta_x}{\partial \theta} + \frac{\partial \beta_\theta}{\partial x}\right),$$

$$\chi_{\theta x} = \chi_{x\theta} = \frac{1}{4}\left(\frac{1}{R^2}\left(\frac{\partial^2 w}{\partial \theta^2} - \frac{\partial v}{\partial \theta}\right) - \frac{\partial^2 w}{\partial x^2} - \frac{1}{R}\frac{\partial \beta_\theta}{\partial \theta} + \frac{\partial \beta_x}{\partial x}\right),$$

$$\chi_{zz} = \frac{1}{2}\left(\frac{1}{R^2}\frac{\partial u}{\partial \theta} - \frac{1}{R}\frac{\partial \beta_x}{\partial \theta} + \frac{\partial \beta_\theta}{\partial x}\right),$$

$$\chi_{\theta x} = \chi_{x\theta} = \frac{1}{4}\left(\frac{1}{R^2}\left(\frac{\partial^2 w}{\partial \theta^2} - \frac{\partial v}{\partial \theta}\right) - \frac{\partial^2 w}{\partial x^2} - \frac{1}{R}\frac{\partial \beta_\theta}{\partial \theta} + \frac{\partial \beta_x}{\partial x}\right),$$

$$\chi_{z\theta} = \chi_{\theta z} = \frac{1}{4R}\begin{pmatrix} \dfrac{\partial^2 v}{\partial x\,\partial\theta} - \dfrac{1}{R}\dfrac{\partial^2 u}{\partial \theta^2} + \dfrac{\partial w}{\partial x} \\ +z\dfrac{\partial^2 \beta_\theta}{\partial x\,\partial\theta} - \dfrac{z}{R}\dfrac{\partial^2 \beta_x}{\partial \theta^2} - \beta_x \end{pmatrix},$$

$$\chi_{zx} = \chi_{xz} = \frac{1}{4}\begin{pmatrix} \dfrac{v}{R^2} - \dfrac{1}{R}\dfrac{\partial^2 u}{\partial \theta\,\partial x} + \dfrac{\partial^2 v}{\partial x^2} \\ -\dfrac{1}{R^2}\dfrac{\partial w}{\partial \theta} + z\dfrac{\partial^2 \beta_\theta}{\partial x^2} - \dfrac{z}{R}\dfrac{\partial^2 \beta_x}{\partial \theta\,\partial x} - \dfrac{\beta_\theta}{R} \end{pmatrix}.$$

Appendix C

Based on Eq. (12), electric field E_i, magnetic field H_i is obtained and also, piezo-magnetic strain tensor B_i and dielectric displacement tensor $D_i$are considered as follow

$$\begin{Bmatrix} E_x \\ E_\theta \\ E_z \end{Bmatrix} = -\begin{Bmatrix} \varphi_{,x} \\ \dfrac{\varphi_{,\theta}}{R} \\ \varphi_{,z} \end{Bmatrix} = \begin{Bmatrix} \dfrac{\partial \varphi}{\partial x}\cos\left(\dfrac{\pi \tilde{z}}{h_p}\right) \\ \dfrac{1}{R}\dfrac{\partial \varphi}{\partial \theta}\cos\left(\dfrac{\pi \tilde{z}}{h_p}\right) \\ -\dfrac{2\varphi_0}{h_p} - \dfrac{\pi}{h_p}\varphi(x,\theta,t)\sin\left(\dfrac{\pi \tilde{z}}{h_p}\right) \end{Bmatrix},$$

$$\begin{Bmatrix} H_x \\ H_\theta \\ H_z \end{Bmatrix} = -\begin{Bmatrix} \psi_{,x} \\ \dfrac{\psi_{,\theta}}{R} \\ \psi_{,z} \end{Bmatrix} = \begin{Bmatrix} \dfrac{\partial \psi}{\partial x}\cos\left(\dfrac{\pi \tilde{z}}{h_p}\right) \\ \dfrac{1}{R}\dfrac{\partial \psi}{\partial \theta}\cos\left(\dfrac{\pi \tilde{z}}{h_p}\right) \\ -\dfrac{2\psi_0}{h_p} - \dfrac{\pi}{h_p}\psi(x,\theta,t)\sin\left(\dfrac{\pi \tilde{z}}{h_p}\right) \end{Bmatrix},$$

$$\begin{Bmatrix} D_x \\ D_\theta \\ D_z \end{Bmatrix} = \begin{bmatrix} 0 & 0 & e_{31} \\ 0 & 0 & e_{32} \\ 0 & e_{24} & 0 \\ e_{15} & 0 & 0 \\ 0 & 0 & 0 \end{bmatrix}^T \begin{Bmatrix} \varepsilon_{xx} \\ \varepsilon_{\theta\theta} \\ \gamma_{z\theta} \\ \gamma_{zx} \\ \gamma_{x\theta} \end{Bmatrix} + \begin{bmatrix} k_{11} & 0 & 0 \\ 0 & k_{22} & 0 \\ 0 & 0 & k_{33} \end{bmatrix} \begin{Bmatrix} E_x \\ E_\theta \\ E_z \end{Bmatrix} + \begin{bmatrix} g_{11} & 0 & 0 \\ 0 & g_{22} & 0 \\ 0 & 0 & g_{33} \end{bmatrix} \begin{Bmatrix} H_x \\ H_\theta \\ H_z \end{Bmatrix},$$

$$\begin{Bmatrix} B_x \\ B_\theta \\ B_z \end{Bmatrix} = \begin{bmatrix} 0 & 0 & q_{31} \\ 0 & 0 & q_{32} \\ 0 & q_{24} & 0 \\ q_{15} & 0 & 0 \\ 0 & 0 & 0 \end{bmatrix}^T \begin{Bmatrix} \varepsilon_{xx} \\ \varepsilon_{\theta\theta} \\ \gamma_{z\theta} \\ \gamma_{zx} \\ \gamma_{x\theta} \end{Bmatrix} + \begin{bmatrix} g_{11} & 0 & 0 \\ 0 & g_{22} & 0 \\ 0 & 0 & g_{33} \end{bmatrix} \begin{Bmatrix} E_x \\ E_\theta \\ E_z \end{Bmatrix} + \begin{bmatrix} \mu_{11} & 0 & 0 \\ 0 & \mu_{22} & 0 \\ 0 & 0 & \mu_{33} \end{bmatrix} \begin{Bmatrix} H_x \\ H_\theta \\ H_z \end{Bmatrix}.$$

Appendix D

The resultants forces and moments, some other parameters related to material length scale parameter, electric and magnetic fields are defined as the following form (Mohammadimehr *et al.* 2016b)

$$\{N_{xx}, N_{\theta\theta}, N_{x\theta}\} = \int_{-h_b-\frac{h_c}{2}}^{h_t+\frac{h_c}{2}} \{\sigma_{xx}, \sigma_{\theta\theta}, \sigma_{x\theta}\}\mathrm{d}z\,,$$

$$\{M_{xx}, M_{\theta\theta}, M_{x\theta}\} = \int_{-h_b-\frac{h_c}{2}}^{h_t+\frac{h_c}{2}} \{\sigma_{xx}, \sigma_{\theta\theta}, \sigma_{x\theta}\}z\mathrm{d}z\,,$$

$$\{Q_x, Q_\theta\} = \int_{-h_b-\frac{h_c}{2}}^{h_t+\frac{h_c}{2}} \{\sigma_{xz}, \sigma_{\theta z}\}\mathrm{d}z\,,$$

$$\{T_{xx}, T_{\theta\theta}, T_{zz}, T_{z\theta}, T_{zx}, T_{\theta x}\} = \int_{-h_b-\frac{h_c}{2}}^{h_t+\frac{h_c}{2}} \{m_{xx}, m_{\theta\theta}, m_{zz}, m_{z\theta}, m_{zx}, m_{\theta x}\}\, z\mathrm{d}z,$$

$$\begin{Bmatrix} P_x \\ P_\theta \\ P_z \end{Bmatrix} = \int_{-h_b-\frac{h_c}{2}}^{h_t+\frac{h_c}{2}} \begin{Bmatrix} D_x\cos\left(\dfrac{\pi \tilde{z}}{h_p}\right) \\ \dfrac{D_\theta}{R}\cos\left(\dfrac{\pi \tilde{z}}{h_p}\right) \\ D_x\left(\dfrac{\pi}{h_p}\right)\cos\left(\dfrac{\pi \tilde{z}}{h_p}\right) \end{Bmatrix}\mathrm{d}z,$$

$$\begin{Bmatrix} O_x \\ O_\theta \\ O_z \end{Bmatrix} = \int_{-h_b-\frac{h_c}{2}}^{h_t+\frac{h_c}{2}} \begin{Bmatrix} B_x\cos\left(\dfrac{\pi \tilde{z}}{h_p}\right) \\ \dfrac{B_\theta}{R}\cos\left(\dfrac{\pi \tilde{z}}{h_p}\right) \\ B_x\left(\dfrac{\pi}{h_p}\right)\cos\left(\dfrac{\pi \tilde{z}}{h_p}\right) \end{Bmatrix}\mathrm{d}z,$$

$$\{Y_{xx}, Y_{\theta\theta}, Y_{zz}, Y_{z\theta}, Y_{zx}, Y_{\theta x}\} = \int_{-h_b-\frac{h_c}{2}}^{h_t+\frac{h_c}{2}} \{m_{xx}, m_{\theta\theta}, m_{zz}, m_{z\theta}, m_{zx}, m_{\theta x}\}\,\mathrm{d}z.$$

Appendix E

Using Eqs. (12)-(14) and Hamilton's principle, the governing equations based on displacement are derived in Appendix E.

$$\begin{aligned}
\delta u_1:\ & -\left(D_{1,0}+A_{20}\right)\frac{\partial^2 u_1}{\partial x^2}+\frac{D_{5,0}l^2}{4R^2}\frac{\partial^4 u_1}{\partial x^2\,\partial\theta^2}-\frac{D_{5,0}l^2}{R^4}\frac{\partial^2 u_1}{\partial\theta^2}\\
&-\frac{1}{R^2}\left(D_{5,0}+C_{20}\right)\frac{\partial^2 u_1}{\partial\theta^2}+\frac{D_{5,0}l^2}{4R^4}\frac{\partial^4 u_1}{\partial\theta^4}\\
&-\frac{D_{5,0}l^2}{4R}\frac{\partial^4 v_1}{\partial x^3\,\partial\theta}+\frac{1}{R}\left(\frac{D_{5,0}l^2}{4R^2}\right)\frac{\partial^2 v_1}{\partial x\,\partial\theta}\\
&-\frac{1}{R}\left(D_{3,0}+D_{5,0}+B_{20}+C_{20}\right)\frac{\partial^2 v_1}{\partial x\,\partial\theta}\\
&-\frac{D_{5,0}l^2}{4R^3}\frac{\partial^4 v_1}{\partial x\,\partial\theta^3}-\frac{D_{3,0}+B_{20}}{R}\frac{\partial w_1}{\partial x}-\frac{D_{5,0}l^2}{2R^3}\frac{\partial^3 w_1}{\partial x\,\partial\theta^2}\\
&-\frac{1}{R}\left(\frac{D_{5,0}l^2}{4R}-\frac{D_{5,1}l^2}{2R^2}\right)\frac{\partial^2\beta_{\theta_1}}{\partial x\,\partial\theta}\\
&-\frac{D_{3,1}+D_{5,1}+B_{21}+C_{21}}{R}\frac{\partial^2\beta_{\theta1}}{\partial x\,\partial\theta}+\frac{5D_{5,0}l^2}{4R^3}\frac{\partial^2\beta_{x1}}{\partial\theta^2}\\
&-\frac{1}{R^2}\left(C_{21}+D_{5,1}\right)\frac{\partial^2\beta_{x1}}{\partial\theta^2}-\left(D_{1,1}+A_{21}\right)\frac{\partial^2\beta_{x1}}{\partial x^2}\\
&-\frac{D_{5,1}l^2}{4R^3}\frac{\partial^4\beta_{\theta1}}{\partial x\,\partial\theta^3}+\frac{D_{5,1}l^2}{4R^4}\frac{\partial^4\beta_{x1}}{\partial\theta^4}-\frac{D_{5,1}l^2}{4R}\frac{\partial^4\beta_{\theta1}}{\partial x^3\,\partial\theta}\\
&+\frac{D_{5,1}l^2}{4R^2}\frac{\partial^4\beta_{x1}}{\partial x^2\,\partial\theta^2}+\frac{\partial}{\partial x}(\alpha_{11}\Delta T+\beta_{11}\Delta H)D_{1,0}\\
&+\frac{\partial}{\partial x}(\alpha_{22}\Delta T+\beta_{22}\Delta H)D_{3,0}-\frac{\partial N_{1,\varphi_0}}{\partial x}-\frac{\partial N_{1,\psi_0}}{\partial x}\\
&-N_{1,\varphi}\frac{\partial\varphi_1}{\partial x}-N_{1,\psi}\frac{\partial\psi_1}{\partial x}+I^{(1)}\frac{\partial^2\beta_{x1}}{\partial t^2}+I^{(0)}\frac{\partial^2 u_1}{\partial t^2}=0,
\end{aligned}\tag{E-1}$$

$$\begin{aligned}
\delta v_1:\ & \frac{D_{5,0}l^2}{4}\frac{\partial^4 v_1}{\partial x^4}-\frac{D_{5,0}l^2}{2R^2}\frac{\partial^2 v_1}{\partial x^2}-\left(D_{5,0}-C_{20}\right)\frac{\partial^2 v_1}{\partial x^2}\\
&-\frac{D_{5,0}l^2}{4R^4}\frac{\partial^2 v_1}{\partial\theta^2}-\frac{1}{R^2}\left(D_{2,0}+A_{20}\right)\frac{\partial^2 v_1}{\partial\theta^2}+\frac{D_{5,0}l^2}{4R^2}\frac{\partial^4 v_1}{\partial x^2\,\partial\theta^2}\\
&+\frac{1}{R^2}\left(\frac{D_{5,0}l^2}{4R^2}+D_{4,0}k_s\right)v_1-\frac{D_{5,0}l^2}{4R}\frac{\partial^4 u_1}{\partial x^3\,\partial\theta}\\
&-\frac{D_{5,0}l^2}{4R^3}\frac{\partial^4 u_1}{\partial x\,\partial\theta^3}+\frac{1}{R}\left(\frac{D_{5,0}l^2}{4R^2}-D_{3,0}-D_{5,0}\right)\frac{\partial^2 u_1}{\partial x\,\partial\theta}\\
&+\frac{3D_{5,0}l^2}{4R^2}\frac{\partial^3 w_1}{\partial x^2\,\partial\theta}+\frac{D_{5,0}l^2}{4R^4}\frac{\partial^3 w_1}{\partial\theta^3}\\
&-\frac{1}{R^2}\left(D_{2,0}+\frac{D_{5,0}l^2}{4R^2}+D_{4,0}k_s\right)\frac{\partial w_1}{\partial\theta}\\
&-\frac{1}{R}\left(\frac{D_{5,0}l^2}{2R}+D_{5,1}+D_{3,1}+\frac{D_{5,1}l^2}{4R^2}\right)\frac{\partial^2\beta_{x1}}{\partial x\,\partial\theta}\\
&-\frac{1}{R^2}\left(\frac{D_{5,0}l^2}{4R}+D_{2,1}\right)\frac{\partial^2\beta_{\theta1}}{\partial\theta^2}\\
&-\left(\frac{3D_{5,0}l^2}{4R}+D_{5,1}+\frac{D_{5,1}l^2}{4R^2}\right)\frac{\partial^2\beta_{\theta1}}{\partial x^2}+\frac{D_{5,1}l^2}{4R^2}\frac{\partial^4\beta_{\theta1}}{\partial x^2\,\partial\theta^2}\\
&-\frac{D_{5,1}l^2}{4R^3}\frac{\partial^4\beta_{x1}}{\partial x\,\partial\theta^3}+\frac{D_{5,1}l^2}{4}\frac{\partial^4\beta_{\theta1}}{\partial x^4}\\
&-\frac{1}{R}\left(\frac{D_{5,0}l^2}{4R^2}+D_{4,0}k_s\right)\beta_{\theta1}-\frac{D_{5,1}l^2}{4R}\frac{\partial^4\beta_{x1}}{\partial x^3\,\partial\theta}\\
&-\frac{1}{R}\left(\frac{\partial N_{2,\varphi_0}}{\partial\theta}+\frac{\partial N_{2,\psi_0}}{\partial\theta}\right)-\frac{1}{R}\left(N_{2,\varphi}\frac{\partial\varphi_1}{\partial\theta}+N_{2,\psi}\frac{\partial\psi_1}{\partial\theta}\right)\\
&-\frac{1}{R}\left(-N_{4,\varphi}\frac{\partial\varphi_1}{\partial\theta}-N_{4,\psi}\frac{\partial\psi_1}{\partial\theta}\right)\\
&0+I^{(1)}\frac{\partial^2\beta_{\theta1}}{\partial t^2}+I^{(0)}\frac{\partial^2 v_1}{\partial t^2}=0,
\end{aligned}\tag{E-2}$$

$$\begin{aligned}
\delta w_1:\ & \frac{D_{5,0}l^2}{4}\frac{\partial^4 w_1}{\partial x^4}-D_{5,0}\left(\frac{l^2}{4R^2}+k_s\right)\frac{\partial^2 w_1}{\partial x^2}+\frac{D_{5,0}l^2}{2R^2}\frac{\partial^4 w_1}{\partial x^2\,\partial\theta^2}\\
&+\frac{D_{5,0}l^2}{4R^4}\frac{\partial^4 w_1}{\partial\theta^4}-\frac{1}{R^2}\left(\frac{D_{5,0}l^2}{4R^2}+D_{4,0}k_s\right)\frac{\partial^2 w_1}{\partial\theta^2}+\frac{D_{2,0}}{R^2}w_1\\
&+\frac{D_{3,0}}{R}\frac{\partial u_1}{\partial x}+\frac{D_{5,0}l^2}{2R^3}\frac{\partial^3 u_1}{\partial x\,\partial\theta^2}-\frac{3D_{5,0}l^2}{4R^2}\frac{\partial^3 v_1}{\partial x^2\,\partial\theta}\\
&+\frac{1}{R^2}\left(D_{2,0}+\frac{D_{5,0}l^2}{4R^2}+D_{4,0}k_s\right)\frac{\partial v_1}{\partial\theta}-\frac{D_{5,0}l^2}{4R^4}\frac{\partial^3 v_1}{\partial\theta^3}\\
&-\frac{D_{5,0}l^2}{4R^2}\frac{\partial^3\beta_{x1}}{\partial x\,\partial\theta^2}-\frac{D_{5,0}l^2}{4}\frac{\partial^3\beta_{x1}}{\partial x^3}\\
&+\left(\frac{D_{5,0}l^2}{4R^2}-D_{5,0}k_s+\frac{D_{3,1}}{R}\right)\frac{\partial\beta_{x1}}{\partial x}-\frac{D_{5,0}l^2}{4R^3}\frac{\partial^3\beta_{\theta1}}{\partial\theta^3}\\
&-\frac{1}{R}\left(\frac{D_{5,0}l^2}{4R^2}+D_{4,0}k_s-\frac{D_{2,1}}{R}\right)\frac{\partial\beta_{\theta1}}{\partial\theta}\\
&-\frac{1}{2R}\left(\frac{D_{5,0}l^2}{2}+\frac{D_{5,1}l^2}{R}\right)\frac{\partial^3\beta_{\theta1}}{\partial x^2\,\partial\theta}\\
&-\frac{1}{R}(\alpha_{11}\Delta T+\beta_{11}\Delta H)D_{3,0}-\frac{1}{R^2}(\alpha_{22}\Delta T+\beta_{22}\Delta H)D_{2,0})\\
&+\frac{1}{R}\left(N_{2,\varphi_0}+N_{2,\varphi}\varphi_1+N_{2,\psi_0}+N_{2,\psi}\psi_1\right)+\frac{1}{R}N_{4,\varphi}\frac{\partial^2\varphi_1}{\partial\theta^2}\\
&+\frac{1}{R}N_{4,\psi}\frac{\partial^2\psi_1}{\partial\theta^2}+N_{5,\varphi}\frac{\partial^2\varphi_1}{\partial x^2}+N_{5,\psi}\frac{\partial^2\psi_1}{\partial x^2}+I^{(0)}\frac{\partial^2 w_1}{\partial t^2}\\
&-q(x,\theta)+K_{W_1}w_1-K_{W_2}(w_2-w_1)\\
&-K_{G_1}\nabla^2 w_1+K_{G_2}\nabla^2(w_2-w_1)=0,
\end{aligned}\tag{E-3}$$

$$\begin{aligned}
\delta\beta_{x_1}:\ & -\frac{D_{5,0}l^2}{4}\frac{\partial^2\beta_{x1}}{\partial x^2}-\left(D_{1,2}+A_{22}\right)\frac{\partial^2\beta_{x1}}{\partial x^2}+\frac{D_{5,2}l^2}{4R^2}\frac{\partial^4\beta_{x1}}{\partial x^2\,\partial\theta^2}\\
&+\frac{D_{5,2}l^2}{4R^4}\frac{\partial^4\beta_{x1}}{\partial\theta^4}-\frac{1}{R^2}\left(D_{5,0}l^2-\frac{D_{5,1}l^2}{2R}\right)\frac{\partial^2\beta_{x1}}{\partial\theta^2}\\
&-\frac{1}{R^2}\left(D_{5,2}+C_{22}\right)\frac{\partial^2\beta_{x1}}{\partial\theta^2}+\frac{D_{5,0}l^2}{4R^2}\beta_{x1}\\
&+\left(D_{5,0}k_s+C_{20}\right)\beta_{x1}+\frac{1}{R}\left(\frac{3D_{5,0}l^2}{4}-\frac{D_{5,1}l^2}{2R}\right)\frac{\partial^2\beta_{\theta1}}{\partial x\,\partial\theta}\\
&-\frac{1}{R}\left(D_{3,2}+D_{5,2}+C_{22}+B_{22}\right)\frac{\partial^2\beta_{\theta1}}{\partial x\,\partial\theta}-\frac{D_{5,2}l^2}{4R^3}\frac{\partial^4\beta_{\theta1}}{\partial x\,\partial\theta^3}\\
&-\frac{D_{5,2}l^2}{4R}\frac{\partial^4\beta_{\theta1}}{\partial x^3\,\partial\theta}+\frac{5D_{5,0}l^2}{4R^3}\frac{\partial^2 u_1}{\partial\theta^2}\\
&-\frac{1}{R^2}\left(D_{5,1}+C_{21}\right)\frac{\partial^2 u_1}{\partial\theta^2}-\frac{1}{R}\left(\frac{D_{5,0}l^2}{2R}+\frac{D_{5,1}l^2}{4R^2}\right)\frac{\partial^2 v_1}{\partial x\,\partial\theta}\\
&-\frac{1}{R}\left(+D_{3,1}+D_{5,1}+C_{21}+B_{21}\right)\frac{\partial^2 v_1}{\partial x\,\partial\theta}\\
&+\frac{D_{5,0}l^2}{4}\frac{\partial^3 w_1}{\partial x^3}+\frac{D_{5,0}l^2}{4R^2}\frac{\partial^3 w_1}{\partial x\,\partial\theta^2}-\frac{D_{5,0}l^2}{4R^2}\frac{\partial w_1}{\partial x}\\
&+(D_{5,0}k_s-\frac{D_{3,1}}{R}+C_{20}-\frac{1}{R}B_{21})\frac{\partial w_1}{\partial x}-\frac{D_{5,1}l^2}{4R^3}\frac{\partial^4 v_1}{\partial x\,\partial\theta^3}\\
&-\left(D_{1,1}+A_{21}\right)\frac{\partial^2 u_1}{\partial x^2}+\frac{D_{5,1}l^2}{4R^4}\frac{\partial^4 u_1}{\partial\theta^4}+\frac{D_{5,1}l^2}{4R^2}\frac{\partial^4 u_1}{\partial x^2\,\partial\theta^2}\\
&-\frac{D_{5,1}l^2}{4R}\frac{\partial^4 v_1}{\partial x^3\,\partial\theta}-\frac{\partial M_{1,\varphi_0}}{\partial x}-\frac{\partial M_{1,\psi_0}}{\partial x}\\
&-M_{1,\varphi}\frac{\partial\varphi_1}{\partial x}-M_{1,\psi}\frac{\partial\psi_1}{\partial x}-N_{5,\varphi}\frac{\partial\varphi_1}{\partial x}-N_{5,\psi}\frac{\partial\psi_1}{\partial x}\\
&+I^{(2)}\frac{\partial^2\beta_{x_1}}{\partial t^2}+I^{(1)}\frac{\partial^2 u_1}{\partial t^2}=0,
\end{aligned}\tag{E-4}$$

$$
\begin{aligned}
\delta\beta_{\theta_1}:\ & \frac{D_{5,2}l^2}{4}\frac{\partial^4\beta_{\theta1}}{\partial x^4}-\left(D_{5,0}l^2+\frac{D_{5,2}l^2}{2R^2}+\frac{D_{5,1}l^2}{2R}\right)\frac{\partial^2\beta_{\theta1}}{\partial x^2}\\
&-M_{1,\varphi}\frac{\partial\varphi_1}{\partial x}-\left(D_{5,2}+C_{22}\right)\frac{\partial^2\beta_{\theta1}}{\partial x^2}+\frac{D_{5,2}l^2}{4R^2}\frac{\partial^4\beta_{\theta1}}{\partial x^2\,\partial\theta^2}\\
&+\frac{D_{5,1}l^2}{4}\frac{\partial^4 v_1}{\partial x^4}-\frac{D_{5,0}l^2}{4R^2}\frac{\partial^2\beta_{\theta_1}}{\partial\theta^2}-\frac{1}{R^2}\left(D_{2,2}+A_{22}\right)\frac{\partial^2\beta_{\theta_1}}{\partial\theta^2}\\
&+\frac{1}{R}\left(\frac{3D_{5,0}l^2}{4}-\frac{D_{5,1}l^2}{2R}\right)\frac{\partial^2\beta_{x_1}}{\partial x\,\partial\theta}\\
&-\frac{D_{3,2}+D_{5,2}+B_{22}+C_{22}}{R}\frac{\partial^2\beta_{x1}}{\partial x\,\partial\theta}-\frac{D_{5,1}l^2}{4R^3}\frac{\partial^4 u_1}{\partial x\,\partial\theta^3}\\
&-\frac{D_{5,2}l^2}{4R^3}\frac{\partial^4\beta_{x_1}}{\partial x\,\partial\theta^3}-\frac{D_{5,2}l^2}{4R}\frac{\partial^4\beta_{x_1}}{\partial x^3\,\partial\theta}\\
&-\left(\frac{D_{5,0}l^2}{4R^2}-\frac{D_{5,1}l^2}{2R^3}\right)\frac{\partial^2 u_1}{\partial x\,\partial\theta}\\
&-\frac{D_{3,1}+D_{5,1}+B_{21}+C_{21}}{R}\frac{\partial^2 u_1}{\partial x\,\partial\theta}-\frac{D_{5,0}l^2}{4R^3}v_1\\
&-\left(\frac{3D_{5,0}l^2}{4R}+\frac{D_{5,1}l^2}{4R^2}\right)\frac{\partial^2 v_1}{\partial x^2}-\left(D_{5,1}+C_{21}\right)\frac{\partial^2 v_1}{\partial x^2}\\
&-\frac{1}{R^2}\left(\frac{D_{5,0}l^2}{4R}\right)\frac{\partial^2 v_1}{\partial\theta^2}-\frac{1}{R^2}\left(D_{2,1}+A_{21}\right)\frac{\partial^2 v_1}{\partial\theta^2}\\
&+\frac{D_{5,1}l^2}{4R^2}\frac{\partial^4 v_1}{\partial x^2\,\partial\theta^2}-\frac{1}{R}\left(C_{20}+k_sD_{4,0}\right)v_1\\
&+\frac{1}{R}\left(\frac{D_{5,0}l^2}{4}+\frac{D_{5,1}l^2}{2R}\right)\frac{\partial^3 w_1}{\partial x^2\,\partial\theta}+\frac{D_{5,0}l^2}{4R^3}\frac{\partial^3 w_1}{\partial\theta^3}\\
&+\frac{1}{R}\left(\frac{D_{5,0}l^2}{4R^2}\right)\frac{\partial w_1}{\partial\theta}-\frac{D_{5,1}l^2}{4R}\frac{\partial^4 u_1}{\partial x^3\,\partial\theta}\\
&+\frac{1}{R}\left(k_sD_{4,0}-\frac{D_{2,1}}{R}+C_{20}-\frac{A_{2,1}}{R}\right)\frac{\partial w_1}{\partial\theta}+\frac{D_{5,0}l^2}{4R^2}\beta_{\theta_1}\\
&+\left(k_sD_{4,0}+C_{20}\right)\beta_{\theta_1}-\frac{1}{R}\left(\frac{\partial M_{2,\varphi_0}}{\partial\theta}+\frac{\partial M_{2,\psi_0}}{\partial\theta}\right)\\
&-\frac{1}{R}M_{2,\varphi}\frac{\partial\varphi_1}{\partial\theta}-\frac{1}{R}M_{2,\psi}\frac{\partial\psi_1}{\partial\theta}-N_{4,\varphi}\frac{\partial\varphi_1}{\partial\theta}-N_{4,\psi}\frac{\partial\psi_1}{\partial\theta}\\
&+I^{(1)}\frac{\partial^2 v_1}{\partial t^2}+I^{(2)}\frac{\partial^2\beta_{\theta1}}{\partial t^2}=0,
\end{aligned}
\tag{E-5}
$$

$$
\begin{aligned}
\delta\varphi_1:\ & N_{5,\varphi}\left(\frac{\partial^2 w_1}{\partial x^2}+\frac{\partial\beta_{x1}}{\partial x}\right)+N_{1,D}\frac{\partial^2\varphi_1}{\partial x^2}+N_{1,B}\frac{\partial^2\psi_1}{\partial x^2}\\
&+N_{4,\varphi}\left(\frac{1}{R}\frac{\partial^2 w_1}{\partial\theta^2}+\frac{\partial\beta_{\theta1}}{\partial\theta}-\frac{1}{R}\frac{\partial v_1}{\partial\theta}\right)+N_{2,B}\frac{\partial^2\varphi_1}{\partial\theta^2}\\
&+N_{2,D}\frac{\partial^2\psi_1}{\partial\theta^2}+N_{1,\varphi}\frac{\partial u_1}{\partial x}+M_{1,\varphi}\frac{\partial\beta_{x1}}{\partial x}\\
&+\frac{1}{R}N_{2,\varphi}\left(w_1+\frac{\partial v_1}{\partial\theta}\right)+M_{2,\varphi}\frac{\partial\beta_{\theta1}}{\partial\theta}\\
&-N_{3,D1}\varphi_0-N_{3,D}\varphi_1-N_{3,B1}\varphi_0-N_{3,B}\varphi_1=0,
\end{aligned}
\tag{E-6}
$$

$$
\begin{aligned}
\delta\psi_1:\ & N_{5,\psi}\left(\frac{\partial^2 w_1}{\partial x^2}+\frac{\partial\beta_{x1}}{\partial x}\right)+N_{1,B}\frac{\partial^2\varphi_1}{\partial x^2}+N_{1,B1}\frac{\partial^2\psi_1}{\partial x^2}\\
&+N_{4,\psi}\left(\frac{1}{R}\frac{\partial^2 w_1}{\partial\theta^2}+\frac{\partial\beta_{\theta1}}{\partial\theta}-\frac{1}{R}\frac{\partial v_1}{\partial\theta}\right)+N_{2,D}\frac{\partial^2\varphi_1}{\partial\theta^2}\\
&+N_{2,B1}\frac{\partial^2\psi_1}{\partial\theta^2}+N_{1,\psi}\frac{\partial u_1}{\partial x}+M_{1,\psi}\frac{\partial\beta_{x1}}{\partial x}\\
&+\frac{1}{R}N_{2,\psi}\left(w_1+\frac{\partial v_1}{\partial\theta}\right)+M_{2,\psi}\frac{\partial\beta_{\theta1}}{\partial\theta}\\
&-N_{3,B1}\varphi_0-N_{3,B}\varphi_1-N_{3,D2}\psi_0-N_{3,B2}\psi_1=0,
\end{aligned}
\tag{E-7}
$$

$$
\begin{aligned}
\delta u_2:\ & -\left(D_{1,0}+A_{20}\right)\frac{\partial^2 u_2}{\partial x^2}+\frac{D_{5,0}l^2}{4R^2}\frac{\partial^4 u_2}{\partial x^2\,\partial\theta^2}-\frac{D_{5,0}l^2}{R^4}\frac{\partial^2 u_2}{\partial\theta^2}\\
&-\frac{1}{R^2}\left(D_{5,0}+C_{20}\right)\frac{\partial^2 u_2}{\partial\theta^2}+\frac{D_{5,0}l^2}{4R^4}\frac{\partial^4 u_2}{\partial\theta^4}-\frac{D_{5,0}l^2}{4R}\frac{\partial^4 v_2}{\partial x^3\,\partial\theta}\\
&+\frac{D_{5,0}l^2}{4R^3}\frac{\partial^2 v_2}{\partial x\,\partial\theta}-\frac{D_{3,0}+D_{5,0}+B_{20}+C_{20}}{R}\frac{\partial^2 v_2}{\partial x\,\partial\theta}\\
&-\frac{D_{5,0}l^2}{4R^3}\frac{\partial^4 v_2}{\partial x\,\partial\theta^3}-\frac{D_{3,0}+B_{20}}{R}\frac{\partial w_2}{\partial x}-\frac{D_{5,0}l^2}{2R^3}\frac{\partial^3 w_2}{\partial x\,\partial\theta^2}\\
&-\frac{1}{R}\left(\frac{D_{5,0}l^2}{4R}-\frac{D_{5,1}l^2}{2R^2}\right)\frac{\partial^2\beta_{\theta_2}}{\partial x\,\partial\theta}\\
&-\frac{D_{3,1}+D_{5,1}+B_{21}+C_{21}}{R}\frac{\partial^2\beta_{\theta2}}{\partial x\,\partial\theta}+\frac{5D_{5,0}l^2}{4R^3}\frac{\partial^2\beta_{x2}}{\partial\theta^2}\\
&-\frac{1}{R^2}\left(C_{21}+D_{5,1}\right)\frac{\partial^2\beta_{x2}}{\partial\theta^2}-\left(D_{1,1}+A_{21}\right)\frac{\partial^2\beta_{x2}}{\partial x^2}\\
&-\frac{D_{5,1}l^2}{4R^3}\frac{\partial^4\beta_{\theta2}}{\partial x\,\partial\theta^3}+\frac{D_{5,1}l^2}{4R^4}\frac{\partial^4\beta_{x2}}{\partial\theta^4}-\frac{D_{5,1}l^2}{4R}\frac{\partial^4\beta_{\theta2}}{\partial x^3\,\partial\theta}\\
&+\frac{D_{5,1}l^2}{4R^2}\frac{\partial^4\beta_{x2}}{\partial x^2\,\partial\theta^2}+\frac{\partial}{\partial x}(\alpha_{11}\Delta T+\beta_{11}\Delta H)D_{1,0}\\
&+\frac{\partial}{\partial x}(\alpha_{22}\Delta T+\beta_{22}\Delta H)D_{3,0}-\frac{\partial N_{1,\varphi_0}}{\partial x}-\frac{\partial N_{1,\psi_0}}{\partial x}\\
&-N_{1,\varphi}\frac{\partial\varphi_2}{\partial x}-N_{1,\psi}\frac{\partial\psi_2}{\partial x}+I^{(1)}\frac{\partial^2\beta_{x2}}{\partial t^2}+I^{(0)}\frac{\partial^2 u_2}{\partial t^2}=0,
\end{aligned}
\tag{E-8}
$$

$$
\begin{aligned}
\delta v_2:\ & \frac{D_{5,0}l^2}{4}\frac{\partial^4 v_2}{\partial x^4}-\frac{D_{5,0}l^2}{2R^2}\frac{\partial^2 v_2}{\partial x^2}-\left(D_{5,0}-C_{20}\right)\frac{\partial^2 v_2}{\partial x^2}\\
&-\frac{D_{5,0}l^2}{4R^4}\frac{\partial^2 v_2}{\partial\theta^2}-\frac{1}{R^2}\left(D_{2,0}+A_{20}\right)\frac{\partial^2 v_2}{\partial\theta^2}+\frac{D_{5,0}l^2}{4R^2}\frac{\partial^4 v_2}{\partial x^2\,\partial\theta^2}\\
&+\frac{1}{R^2}\left(\frac{D_{5,0}l^2}{4R^2}+D_{4,0}k_s\right)v_2-\frac{D_{5,0}l^2}{4R}\frac{\partial^4 u_2}{\partial x^3\,\partial\theta}\\
&-\frac{D_{5,0}l^2}{4R^3}\frac{\partial^4 u_2}{\partial x\,\partial\theta^3}+\frac{1}{R}\left(\frac{D_{5,0}l^2}{4R^2}-D_{3,0}-D_{5,0}\right)\frac{\partial^2 u_2}{\partial x\,\partial\theta}\\
&+\frac{3D_{5,0}l^2}{4R^2}\frac{\partial^3 w_2}{\partial x^2\,\partial\theta}+\frac{D_{5,0}l^2}{4R^4}\frac{\partial^3 w_2}{\partial\theta^3}\\
&-\frac{1}{R^2}\left(D_{2,0}+\frac{D_{5,0}l^2}{4R^2}+D_{4,0}k_s\right)\frac{\partial w_2}{\partial\theta}\\
&-\frac{1}{R^2}\left(\frac{D_{5,0}l^2}{4R}+D_{2,1}\right)\frac{\partial^2\beta_{\theta2}}{\partial\theta^2}\\
&-\frac{1}{R}\left(\frac{D_{5,0}l^2}{2R}+D_{5,1}+D_{3,1}+\frac{D_{5,1}l^2}{4R^2}\right)\frac{\partial^2\beta_{x2}}{\partial x\,\partial\theta}\\
&-\left(\frac{3D_{5,0}l^2}{4R}+D_{5,1}+\frac{D_{5,1}l^2}{4R^2}\right)\frac{\partial^2\beta_{\theta2}}{\partial x^2}+\frac{D_{5,1}l^2}{4R^2}\frac{\partial^4\beta_{\theta2}}{\partial x^2\,\partial\theta^2}\\
&-\frac{D_{5,1}l^2}{4R^3}\frac{\partial^4\beta_{x2}}{\partial x\,\partial\theta^3}+\frac{D_{5,1}l^2}{4}\frac{\partial^4\beta_{\theta2}}{\partial x^4}\\
&-\frac{1}{R}\left(\frac{D_{5,0}l^2}{4R^2}+D_{4,0}k_s\right)\beta_{\theta2}-\frac{D_{5,1}l^2}{4R}\frac{\partial^4\beta_{x2}}{\partial x^3\,\partial\theta}\\
&-\frac{1}{R}\left(\frac{\partial N_{2,\varphi_0}}{\partial\theta}+\frac{\partial N_{2,\psi_0}}{\partial\theta}\right)-\frac{1}{R}\left(N_{2,\varphi}\frac{\partial\varphi_2}{\partial\theta}+N_{2,\psi}\frac{\partial\psi_2}{\partial\theta}\right)\\
&-\frac{1}{R}\left(-N_{4,\varphi}\frac{\partial\varphi_2}{\partial\theta}-N_{4,\psi}\frac{\partial\psi_2}{\partial\theta}\right)\\
&+I^{(1)}\frac{\partial^2\beta_{\theta2}}{\partial t^2}+I^{(0)}\frac{\partial^2 v_2}{\partial t^2}=0,
\end{aligned}
\tag{E-9}
$$

$$
\begin{aligned}
\delta w_2:\ & \frac{D_{5,0}l^2}{4}\frac{\partial^4 w_2}{\partial x^4} - D_{5,0}\left(\frac{l^2}{4R^2}+k_s\right)\frac{\partial^2 w_2}{\partial x^2} + \frac{D_{5,0}l^2}{2R^2}\frac{\partial^4 w_2}{\partial x^2\,\partial\theta^2} \\
& + \frac{D_{5,0}l^2}{4R^4}\frac{\partial^4 w_2}{\partial\theta^4} - \frac{1}{R^2}\left(\frac{D_{5,0}l^2}{4R^2}+D_{4,0}k_s\right)\frac{\partial^2 w_2}{\partial\theta^2} + \frac{D_{2,0}}{R^2}w_2 \\
& + \frac{D_{3,0}}{R}\frac{\partial u_2}{\partial x} + \frac{D_{5,0}l^2}{2R^3}\frac{\partial^3 u_2}{\partial x\,\partial\theta^2} - \frac{3D_{5,0}l^2}{4R^2}\frac{\partial^3 v_2}{\partial x^2\,\partial\theta} \\
& + \frac{1}{R^2}\left(D_{2,0}+\frac{D_{5,0}l^2}{4R^2}+D_{4,0}k_s\right)\frac{\partial v_2}{\partial\theta} \\
& - \frac{D_{5,0}l^2}{4R^4}\frac{\partial^3 v_2}{\partial\theta^3} - \frac{D_{5,0}l^2}{4R^2}\frac{\partial^3\beta_{x_2}}{\partial x\,\partial\theta^2} - \frac{D_{5,0}l^2}{4}\frac{\partial^3\beta_{x_2}}{\partial x^3} \\
& + \left(\frac{D_{5,0}l^2}{4R^2} - D_{5,0}k_s + \frac{D_{3,1}}{R}\right)\frac{\partial\beta_{x_2}}{\partial x} \\
& - \frac{D_{5,0}l^2}{4R^3}\frac{\partial^3\beta_{\theta 2}}{\partial\theta^3} - \frac{1}{2R}\left(\frac{D_{5,0}l^2}{2}+\frac{D_{5,1}l^2}{R}\right)\frac{\partial^3\beta_{\theta 2}}{\partial x^2\,\partial\theta} \\
& - \frac{1}{R}\left(\frac{D_{5,0}l^2}{4R^2}+D_{4,0}k_s - \frac{D_{2,1}}{R}\right)\frac{\partial\beta_{\theta_2}}{\partial\theta} \\
& - \frac{1}{R}(\alpha_{11}\Delta T + \beta_{11}\Delta H)D_{3,0} - \frac{1}{R^2}(\alpha_{22}\Delta T + \beta_{22}\Delta H)D_{2,0} \\
& - \frac{1}{R}\left(-N_{2,\varphi_0} - N_{2,\varphi}\varphi_2 - N_{2,\psi_0} - N_{2,\psi}\psi_2\right) \\
& + \frac{1}{R}N_{4,\varphi}\frac{\partial^2\varphi_2}{\partial\theta^2} + \frac{1}{R}N_{4,\psi}\frac{\partial^2\psi_2}{\partial\theta^2} + N_{5,\varphi}\frac{\partial^2\varphi_2}{\partial x^2} + N_{5,\psi}\frac{\partial^2\psi_2}{\partial x^2} \\
& + I^{(0)}\frac{\partial^2 w_2}{\partial t^2} - q(x,\theta) + K_{w2}(w_2 - w_1) \\
& - K_{G2}\nabla^2(w_2 - w_1) + K_{w3}w_2 - K_{G3}\nabla^2 w_2 = 0,
\end{aligned}
\tag{E-10}
$$

$$
\begin{aligned}
\delta\beta_{x_2}:\ & -\frac{D_{5,0}l^2}{4}\frac{\partial^2\beta_{x_2}}{\partial x^2} - \left(D_{1,2}+A_{22}\right)\frac{\partial^2\beta_{x_2}}{\partial x^2} + \frac{D_{5,2}l^2}{4R^2}\frac{\partial^4\beta_{x_2}}{\partial x^2\,\partial\theta^2} \\
& + \frac{D_{5,2}l^2}{4R^4}\frac{\partial^4\beta_{x_2}}{\partial\theta^4} - \frac{1}{R^2}\left(D_{5,0}l^2 - \frac{D_{5,1}l^2}{2R}\right)\frac{\partial^2\beta_{x_2}}{\partial\theta^2} \\
& - \frac{1}{R^2}\left(D_{5,2}+C_{22}\right)\frac{\partial^2\beta_{x_2}}{\partial\theta^2} + \frac{D_{5,0}l^2}{4R^2}\beta_{x_2} \\
& + \left(D_{5,0}k_s + C_{20}\right)\beta_{x2} + \frac{1}{R}\left(\frac{3D_{5,0}l^2}{4} - \frac{D_{5,1}l^2}{2R}\right)\frac{\partial^2\beta_{\theta_2}}{\partial x\,\partial\theta} \\
& + \frac{5D_{5,0}l^2}{4R^3}\frac{\partial^2 u_2}{\partial\theta^2} - \frac{D_{3,2}+D_{5,2}+C_{22}+B_{22}}{R}\frac{\partial^2\beta_{\theta 2}}{\partial x\,\partial\theta} \\
& - \frac{D_{5,2}l^2}{4R^3}\frac{\partial^4\beta_{\theta 2}}{\partial x\,\partial\theta^3} - \frac{D_{5,2}l^2}{4R}\frac{\partial^4\beta_{\theta 2}}{\partial x^3\,\partial\theta} - \frac{D_{5,1}+C_{21}}{R^2}\frac{\partial^2 u_2}{\partial\theta^2} \\
& + \frac{D_{5,0}l^2}{4}\frac{\partial^3 w_2}{\partial x^3} + \frac{D_{5,0}l^2}{4R^2}\frac{\partial^3 w_2}{\partial x\,\partial\theta^2} \\
& - \frac{1}{R}\left(\frac{D_{5,0}l^2}{2R} + \frac{D_{5,1}l^2}{4R^2}\right)\frac{\partial^2 v_2}{\partial x\,\partial\theta} \\
& - \frac{D_{3,1}+D_{5,1}+C_{21}+B_{21}}{R}\frac{\partial^2 v_2}{\partial x\,\partial\theta} - \left(D_{1,1}+A_{21}\right)\frac{\partial^2 u_2}{\partial x^2} \\
& - \frac{D_{5,0}l^2}{4R^2}\frac{\partial w_2}{\partial x} - \frac{D_{5,1}l^2}{4R^3}\frac{\partial^4 v_2}{\partial x\,\partial\theta^3} \\
& + \left(D_{5,0}k_s - \frac{D_{3,1}}{R} + C_{20} - \frac{1}{R}B_{21}\right)\frac{\partial w_2}{\partial x} + \frac{D_{5,1}l^2}{4R^4}\frac{\partial^4 u_2}{\partial\theta^4} \\
& + \frac{D_{5,1}l^2}{4R^2}\frac{\partial^4 u_2}{\partial x^2\,\partial\theta^2} - \frac{D_{5,1}l^2}{4R}\frac{\partial^4 v_2}{\partial x^3\,\partial\theta} - \frac{\partial M_{1,\varphi_0}}{\partial x} - \frac{\partial M_{1,\psi_0}}{\partial x} \\
& - M_{1,\varphi}\frac{\partial\varphi_2}{\partial x} - M_{1,\psi}\frac{\partial\psi_2}{\partial x} - N_{5,\varphi}\frac{\partial\varphi_2}{\partial x} - N_{5,\psi}\frac{\partial\psi_2}{\partial x} \\
& + I^{(2)}\frac{\partial^2\beta_{x2}}{\partial t^2} + I^{(1)}\frac{\partial^2 u_2}{\partial t^2} = 0,
\end{aligned}
\tag{E-11}
$$

$$
\begin{aligned}
\delta\beta_{\theta_2}:\ & \frac{D_{5,2}l^2}{4}\frac{\partial^4\beta_{\theta_2}}{\partial x^4} - \left(D_{5,0}l^2 + \frac{D_{5,2}l^2}{2R^2} + \frac{D_{5,1}l^2}{2R}\right)\frac{\partial^2\beta_{\theta_2}}{\partial x^2} \\
& - \left(D_{5,2}+C_{22}\right)\frac{\partial^2\beta_{\theta_2}}{\partial x^2} + \frac{D_{5,2}l^2}{4R^2}\frac{\partial^4\beta_{\theta_2}}{\partial x^2\,\partial\theta^2} + \frac{D_{5,1}l^2}{4}\frac{\partial^4 v_2}{\partial x^4} \\
& - \frac{D_{5,0}l^2}{4R^2}\frac{\partial^2\beta_{\theta_2}}{\partial\theta^2} - \frac{1}{R^2}\left(D_{2,2}+A_{22}\right)\frac{\partial^2\beta_{\theta_2}}{\partial\theta^2} \\
& + \frac{1}{R}\left(\frac{3D_{5,0}l^2}{4} - \frac{D_{5,1}l^2}{2R}\right)\frac{\partial^2\beta_{x_2}}{\partial x\,\partial\theta} \\
& - \frac{D_{3,2}+D_{5,2}+B_{22}+C_{22}}{R}\frac{\partial^2\beta_{x_2}}{\partial x\,\partial\theta} - \frac{D_{5,1}l^2}{4R^3}\frac{\partial^4 u_2}{\partial x\,\partial\theta^3} \\
& - \frac{D_{5,2}l^2}{4R^3}\frac{\partial^4\beta_{x_2}}{\partial x\,\partial\theta^3} - \frac{D_{5,2}l^2}{4R}\frac{\partial^4\beta_{x2}}{\partial x^3\,\partial\theta} \\
& - \frac{1}{R}\left(\frac{D_{5,0}l^2}{4R} - \frac{D_{5,1}l^2}{2R^2}\right)\frac{\partial^2 u_2}{\partial x\,\partial\theta} \\
& - \frac{D_{3,1}+D_{5,1}+B_{21}+C_{21}}{R}\frac{\partial^2 u_2}{\partial x\,\partial\theta} \\
& - \left(\frac{3D_{5,0}l^2}{4R} + \frac{D_{5,1}l^2}{4R^2}\right)\frac{\partial^2 v_2}{\partial x^2} - \left(D_{5,1}+C_{21}\right)\frac{\partial^2 v_2}{\partial x^2} \\
& - \frac{D_{5,0}l^2}{4R^3}\frac{\partial^2 v_2}{\partial\theta^2} - \frac{D_{2,1}+A_{21}}{R^2}\frac{\partial^2 v_2}{\partial\theta^2} - \frac{1}{R}\left(C_{20}+k_sD_{4,0}\right)v_2 \\
& - \frac{D_{5,0}l^2}{4R^3}v_2 + \frac{1}{R}\left(\frac{D_{5,0}l^2}{4} + \frac{D_{5,1}l^2}{2R}\right)\frac{\partial^3 w_2}{\partial x^2\,\partial\theta} + \frac{D_{5,0}l^2}{4R^3}\frac{\partial^3 w_2}{\partial\theta^3} \\
& + \frac{D_{5,0}l^2}{4R^3}\frac{\partial w_2}{\partial\theta} + \frac{1}{R}\left(k_sD_{4,0} - \frac{D_{2,1}}{R} + C_{20} - \frac{A_{2,1}}{R}\right)\frac{\partial w_2}{\partial\theta} \\
& + \frac{D_{5,1}l^2}{4R^2}\frac{\partial^4 v_2}{\partial x^2\,\partial\theta^2} - \frac{D_{5,1}l^2}{4R}\frac{\partial^4 u_2}{\partial x^3\,\partial\theta} + \frac{D_{5,0}l^2}{4R^2}\beta_{\theta_2} \\
& + \left(k_sD_{4,0}+C_{20}\right)\beta_{\theta_2} - \frac{1}{R}\left(\frac{\partial M_{2,\varphi_0}}{\partial\theta} + \frac{\partial M_{2,\psi_0}}{\partial\theta}\right) \\
& - \frac{1}{R}M_{2,\varphi}\frac{\partial\varphi_2}{\partial\theta} - \frac{1}{R}M_{2,\psi}\frac{\partial\psi_2}{\partial\theta} - N_{4,\varphi}\frac{\partial\varphi_2}{\partial\theta} - N_{4,\psi}\frac{\partial\psi_2}{\partial\theta} \\
& + I^{(1)}\frac{\partial^2 v_2}{\partial t^2} + I^{(2)}\frac{\partial^2\beta_{\theta 2}}{\partial t^2} = 0,
\end{aligned}
\tag{E-12}
$$

$$
\begin{aligned}
\delta\varphi_2:\ & N_{5,\varphi}\left(\frac{\partial^2 w_2}{\partial x^2} + \frac{\partial\beta_{x2}}{\partial x}\right) + N_{1,D}\frac{\partial^2\varphi_2}{\partial x^2} + N_{1,B}\frac{\partial^2\psi_2}{\partial x^2} \\
& + N_{4,\varphi}\left(\frac{1}{R}\frac{\partial^2 w_2}{\partial\theta^2} + \frac{\partial\beta_{\theta 2}}{\partial\theta} - \frac{1}{R}\frac{\partial v_2}{\partial\theta}\right) + N_{2,B}\frac{\partial^2\varphi_2}{\partial\theta^2} \\
& + N_{2,D}\frac{\partial^2\psi_2}{\partial\theta^2} + N_{1,\varphi}\frac{\partial u_2}{\partial x} + M_{1,\varphi}\frac{\partial\beta_{x_2}}{\partial x} \\
& + \frac{1}{R}N_{2,\varphi}\left(w_2 + \frac{\partial v_2}{\partial\theta}\right) + M_{2,\varphi}\frac{\partial\beta_{\theta_2}}{\partial\theta} \\
& - N_{3,D1}\varphi_0 - N_{3,D}\varphi_2 - N_{3,B1}\varphi_0 - N_{3,B}\varphi_2 = 0,
\end{aligned}
\tag{E-13}
$$

$$
\begin{aligned}
\delta\psi_2:\ & N_{5,\psi}\left(\frac{\partial^2 w_2}{\partial x^2} + \frac{\partial\beta_{x2}}{\partial x}\right) + N_{1,B}\frac{\partial^2\varphi_2}{\partial x^2} + N_{1,B1}\frac{\partial^2\psi_2}{\partial x^2} \\
& + N_{4,\psi}\left(\frac{1}{R}\frac{\partial^2 w_2}{\partial\theta^2} + \frac{\partial\beta_{\theta_2}}{\partial\theta} - \frac{1}{R}\frac{\partial v_2}{\partial\theta}\right) + N_{2,D}\frac{\partial^2\varphi_2}{\partial\theta^2} \\
& + N_{2,B1}\frac{\partial^2\psi_2}{\partial\theta^2} + N_{1,\psi}\frac{\partial u_2}{\partial x} + M_{1,\psi}\frac{\partial\beta_{x2}}{\partial x} \\
& + \frac{1}{R}N_{2,\psi}\left(w_2 + \frac{\partial v_2}{\partial\theta}\right) + M_{2,\psi}\frac{\partial\beta_{\theta_2}}{\partial\theta} \\
& - N_{3,B_1}\varphi_0 - N_{3,B_2}\varphi_2 - N_{3,D_2}\psi_0 - N_{3,B_2}\psi_2 = 0.
\end{aligned}
\tag{E-14}
$$

Appendix F

Also, the coefficients of Eqs. (E-1) to (E-14) are addressed as follows:

$$\left\{D_{1,i}, D^{\alpha}{}_{1,i}, D^{\beta}{}_{1,i}\right\} = \int_{-\frac{h_c}{2}-h_b}^{\frac{h_c}{2}+h_t} Q_{11}(z) z^i \{1, \alpha_{11}(z)\} \mathrm{d}z,$$

$$\left\{D_{2,i}, D^{\alpha}{}_{4,i}, D^{\beta}{}_{4,i}\right\} = \int_{-\frac{h_c}{2}-h_b}^{\frac{h_c}{2}+h_t} Q_{22}(z) z^i \{1, \alpha_{22}(z)\} \mathrm{d}z,$$

$$\left\{D_{3,i}, D^{\alpha}{}_{2,i}, D^{\beta}{}_{2,i} D^{\alpha}{}_{3,i}, D^{\beta}{}_{3,i}\right\} = \int_{-\frac{h_c}{2}-h_b}^{\frac{h_c}{2}+h_t} Q_{12}(z) z^i \{1, \alpha_{11}(z), \alpha_{22}(z)\} \mathrm{d}z,$$

$$D_{4,i} = \int_{-\frac{h_c}{2}-h_b}^{\frac{h_c}{2}+h_t} Q_{44}(z) z^i \, \mathrm{d}z,$$

$$D_{5,i} = \int_{-\frac{h_c}{2}-h_b}^{\frac{h_c}{2}+h_t} Q_{55}(z) z^i \, \mathrm{d}z,$$

$$\left\{N_{1,\varphi_0}, N_{2,\varphi_0}\right\} = \int \frac{2\varphi_0}{h_p} \{e_{31}, e_{32}\} \mathrm{d}z,$$

$$\left\{N_{1,\psi_0}, N_{2,\psi_0}\right\} = \int \frac{2\psi_0}{h_p} \{q_{31}, q_{32}\} \mathrm{d}z.$$

$$\left\{N_{1,\varphi}, N_{2,\varphi}\right\} = \int \frac{\pi}{h_p} \sin\left(\frac{\pi \tilde{z}}{h_p}\right) \{e_{31}, e_{32}\} \mathrm{d}z,$$

$$\left\{N_{1,\psi}, N_{2,\psi}\right\} = \int \frac{\pi}{h_p} \sin\left(\frac{\pi \tilde{z}}{h_p}\right) \{q_{31}, q_{32}\} \mathrm{d}z,$$

$$\left\{N_{4,\varphi}, N_{5,\varphi}\right\} = \int \cos\left(\frac{\pi \tilde{z}}{h_p}\right) \left\{e_{15}, \frac{1}{R} e_{24}\right\} \mathrm{d}z,$$

$$\left\{N_{4,\psi}, N_{5,\psi}\right\} = \int \cos\left(\frac{\pi \tilde{z}}{h_p}\right) \left\{q_{15}, \frac{1}{R} q_{24}\right\} \mathrm{d}z,$$

$$N_{1,D} = \int \cos^2\left(\frac{\pi \tilde{z}}{h_p}\right) \eta_{11} \mathrm{d}z,$$

$$N_{2,B} = \int \frac{1}{R^2} \cos^2\left(\frac{\pi \tilde{z}}{h_p}\right) \eta_{22} \mathrm{d}z,$$

$$N_{3,D} = \int \eta_{33} \frac{\pi^2}{h_p^2} \sin^2\left(\frac{\pi \tilde{z}}{h_p}\right) \mathrm{d}z,$$

$$\left\{N_{1,B}, N_{2,D}\right\} = \int \cos^2\left(\frac{\pi \tilde{z}}{h_p}\right) \left\{d_{11}, \frac{1}{R^2} d_{22}\right\} \mathrm{d}z,$$

$$N_{3,B} = \int d_{33} \frac{\pi^2}{h_p^2} \sin^2\left(\frac{\pi \tilde{z}}{h_p}\right) \mathrm{d}z,$$

$$\left\{N_{3,B_1}, N_{3,D_1}\right\} = \int \frac{4}{h_p^2} \sin^2\left(\frac{\pi \tilde{z}}{h_p}\right) \{d_{33}, \eta_{33}\} \mathrm{d}z,$$

$$\left\{N_{1,B_1}, N_{2,B_1}\right\} = \int \cos^2\left(\frac{\pi \tilde{z}}{h_p}\right) \left\{\mu_{11}, \frac{1}{R^2} \mu_{22}\right\} \mathrm{d}z,$$

$$N_{3,B2} = \int \mu_{33} \frac{\pi^2}{h_p^2} \sin^2\left(\frac{\pi \tilde{z}}{h_p}\right) \mathrm{d}z,$$

$$N_{3,D2} = \int \mu_{33} \frac{\pi^2}{h_p^2} \sin\left(\frac{\pi \tilde{z}}{h_p}\right) \mathrm{d}z,$$

$$\left\{M_{1,\varphi}, M_{2,\varphi}\right\} = \int \frac{\pi z}{h_p} \sin\left(\frac{\pi \tilde{z}}{h_p}\right) \{e_{31}, e_{32}\} \mathrm{d}z,$$

$$\left\{M_{1,\psi}, M_{2,\psi}\right\} = \int \frac{\pi z}{h_p} \sin\left(\frac{\pi \tilde{z}}{h_p}\right) \{q_{31}, q_{32}\} \mathrm{d}z.$$